

RSC Advances



This is an *Accepted Manuscript*, which has been through the Royal Society of Chemistry peer review process and has been accepted for publication.

Accepted Manuscripts are published online shortly after acceptance, before technical editing, formatting and proof reading. Using this free service, authors can make their results available to the community, in citable form, before we publish the edited article. This *Accepted Manuscript* will be replaced by the edited, formatted and paginated article as soon as this is available.

You can find more information about *Accepted Manuscripts* in the [Information for Authors](#).

Please note that technical editing may introduce minor changes to the text and/or graphics, which may alter content. The journal's standard [Terms & Conditions](#) and the [Ethical guidelines](#) still apply. In no event shall the Royal Society of Chemistry be held responsible for any errors or omissions in this *Accepted Manuscript* or any consequences arising from the use of any information it contains.

**Phenomenological modeling and analysis of gas transport in polyimide
membranes for propylene/propane separation**

Sara Najari^a, Seyed Saeid Hosseini^{a*}, Mohammadreza Omidkhah^a, Nicolas R. Tan^b,

^a Department of Chemical Engineering, Tarbiat Modares University

Tehran, Iran 14115-114

^b Research & Development Dept., HOSSTECH Group,

Singapore 528844

*Corresponding author: [S.S. Hosseini](mailto:S.S.Hosseini); Tel.: +98 21 82883335, Fax: +98 21 8288 4931.

E-mail address: saeid.hosseini@modares.ac.ir

Abstract

Olefins and paraffins are the main building blocks for many products in the petrochemical industry. Various research studies have demonstrated the viability of polyimide membranes for high performance olefin/paraffin separation. Further advancements in this field require having a thorough understanding of both sorptive and diffusive factors of permeation. This research study presents an extensive analysis on using frame of reference/bulk flow and Maxwell-Stefan models in order to elaborate on the transport and prediction of the performance in the case of propylene/propane separation using polyimide membranes. Sorption data of pure gases are utilized to calculate the sorption level of gases in binary mixture. The contributions of kinetic and thermodynamic coupling effects (TCE) are assessed using Maxwell-Stefan approach. Moreover, the dual-mode diffusion coefficients are evaluated and optimized for achieving higher accuracy predictions in the case of binary gas mixture. The results reveal the significant role of thermodynamic compared to kinetic coupling effects in governing the transport properties. In overall, Maxwell-Stephan model with the contribution of TCEs offers improved predictions compared to frame of reference/bulk flow model. The findings highlight the inevitable role of taking into account the prominent interactions of feed components in model development for better prediction of performance and evaluation of propylene/propane separation unit using polyimide membranes.

Keywords: Polyimide membrane, Propylene/Propane separation, Bulk flow model, Maxwell-Stefan model, Thermodynamic coupling effects

1- Introduction

Gas and vapor separation processes have gained much attention in chemical and petrochemical industries due to growing need for high purity chemicals [1, 2]. Nitrogen and helium separation along with oxygen enrichment [3-6], hydrogen separation and purification [7-9], CO₂ removal and natural gas processing [10-12], and hydrocarbon recovery and separation [13-15] comprise main industrial applications of membranes-based technologies.

Separation of light olefins from paraffin gases is of paramount importance in the petrochemical industry due to their applications as raw materials for a wide range of chemicals [16-19]. Compared to the prevalent separation technologies, which are highly energy-intensive, polymeric membranes can offer a low-cost and simple process alternative [5, 13, 16-18, 20-22]. Among the studied polymers, polyimides have attracted much attention due to their chemical resistance, thermal stability and mechanical strength in many gas and vapor separation applications [23-27]. Extensive research on the separation performance of various polymeric membranes for olefin/paraffin separation has indicated the superior characteristics of polyimides compared to the conventional polymers [16, 18, 28-32].

The separation performance in the polyimide membrane is based on the difference in sorption and diffusion of olefin and paraffin molecules. The dual mode sorption model, based on the superposition of the Langmuir model and Henry's law, has been extensively used to represent transport in glassy membranes [33-39]. This model describes permeation of binary gas mixture using sorption data of pure gases, while in binary systems the flux of each component cannot be considered unaffected by each other which was not accounted for in the dual mode model. Some researchers tried to overcome this shortcoming partly by considering the convective flux via applying the frame of reference/bulk flow model [40-44]. Accordingly, using bulk flow model

the permeation of binary gas mixture can be described as a ternary system comprising two penetrants and a membrane. This approach successfully predicted permeation of binary gas mixture through some polyimide membranes while failed in some other cases. Das and Koros [44, 45] analyzed the results of propylene/propane separation by 6FDA-6FpDA with both dual mode and frame of reference/bulk flow model. According to the results, calculated selectivity by dual mode model was higher than the experimental selectivity of binary gas mixture while the results of frame of reference/bulk flow model were in good agreement with them. In contrast, frame of reference /bulk flow model was not able to predict the separation performance of 6FDA-DAM for the same binary gas mixture in the research done by Burns and Koros [43]. Dual mode model overestimated the permeability of propylene in the mentioned study while underestimated that of propane. Moreover, this model deviated dramatically from the experimental selectivity both in the amount and the trend. One probable reason for this discordance may be coupling of the diffusion coefficients which can be investigated through applying Maxwell-Stefan approach in the mixed gas membrane separation [43].

Although the application of the dual mode and frame of reference/bulk flow models were examined in the literature for predicting propylene/propane separation performance in several different membranes, the efficiency of Maxwell-Stefan model has not been assessed yet in the same systems. However, the vast amount of studies on different membrane separation systems utilizing the Maxwell-Stefan model have proved the ability of this approach in overcoming the complications of mass transport in membranes [41, 46-54]. In addition, to the best of our knowledge so far no critical investigation has been reported comparing different approaches of mass transport through polyimide membranes for the separation of propylene/propane binary mixture.

The main objective of the present study is to evaluate and analyze both frame of reference/bulk flow and Maxwell-Stefan models for predicting the permeation and selectivity in polyimide membranes for propylene/propane separation. Besides, the contribution of kinetic and thermodynamic coupling effects were also investigated via employing Maxwell-Stefan model. Moreover, the influence of diffusion coefficients on the model predictions was also assessed and optimized. Sorption data of pure gases from available literature were employed to calculate sorption level of binary gas mixture using dual sorption model. Fluxes and subsequently permeability were calculated using the two mentioned models. The governing transport equations were solved using MATLAB codes.

2- Theory and fundamentals

2-1- Dual mode sorption

Sorption in glassy polymers can be described by the dual mode model which presents two types of sorption modes; one includes the molecularly dissolved mode and the other accounts for non-equilibrium pre-existing gaps or excess volume between chains [34, 55]. Accordingly, sorption isotherm of component “*i*” exhibited the following form [34, 44, 55, 56]:

$$C_i = k_{Di}p_i + \frac{C'_{Hi}b_i p_i}{1 + b_i p_i} \quad (1)$$

where k_{Di} is the Henry's law constant and C'_{Hi} is the Langmuir capacity constant which is an indication of the second sorption mode. The affinity constant, b_i , is the measure of polymer attraction for the sorbed molecule.

Fick's law is the most widespread model that presents a simple relation between the flux of the penetrant and the gradient of its concentration, described according to Eq. (2) [55].

$$J_i = D_i \frac{dC_i}{dz} \quad (2)$$

Dual mode sorption can be extended to represent the behavior of binary gas mixture as follows:

$$C_i = C_{Di} + C_{Hi} = k_{Di}p_i + \frac{C'_{Hi}b_i p_i}{1 + b_i p_i + b_j p_j} \quad (3)$$

where C_{Di} is the Henry concentration and C_{Hi} is the Langmuir concentration.

2-2- Partial immobilization theory

Partial immobilization theory provides a more general form than that of Fick's speculating a finite mobility for the Langmuir sites along with Henry's law sites [55, 57]:

$$J_i = -D_{Di} \frac{dC_{Di}}{dz} - D_{Hi} \frac{dC_{Hi}}{dz} \quad (4)$$

where D_{Di} is the diffusion coefficient of component “*i*” in the Henry's sites and D_{Hi} is the diffusion coefficient of component “*i*” in the Langmuir sites. In most cases, partial immobilization theory gives an appropriate description of mass transport in membrane. However in some cases, it is unable to show the relation between the concentration within the polymer and flux of penetrants [46, 58, 59]. This formulation of diffusion is based on the assumption that diffusion of each molecule is independent of other molecules. However, in several situations such assumption fails to provide an appropriate description of the separation performance [46]. Applying this model along with sorption model leads to the following expression for the permeability of component “*i*” [57].

$$P_i = k_{Di}D_{Di} + \frac{C'_{Hi}D_{Hi}b_i}{1 + b_i p_i} \quad (5)$$

According to the partial immobilization theory, Henry's population is completely mobile and is able to fully participate in performing the diffusive jump while only a fraction of Langmuir's population is able to do so [40]. Therefore, mobile concentration comprises of C_{Di} along with a fraction of C_{Hi} presented according to Eq. (6).

$$C_{Mi} = C_{Di} + F_i C_{Hi} \quad (6)$$

where F_i is the ratio of diffusion coefficients D_{Hi}/D_{Di} [35].

According to Eqs. (4) and (6) the following expression can be written for the flux of component "i" [42]:

$$J_i = D_{Di} \frac{dC_{Mi}}{dz} \quad (7)$$

Since molar volumes of the gaseous penetrants are not readily available, it is more convenient to express equations in mass units. Therefore, the mobile concentration (g/g pol.) also known as "sorption level" is defined as follows:

$$w_i = C_{Mi} \frac{Mw_i}{22400\rho} \quad (8)$$

where Mw is the molecular weight of each component and ρ is the density of membrane.

Employing Eqs. (6) and (8) leads to the following expression for the mobile concentration [44]:

$$w_i = w_{Di} + F_i w_{Hi} = \left(\frac{Mw_i}{22400\rho} k_{Di} p_i + \frac{Mw_i}{22400\rho} \frac{F_i C'_{Hi} b_i p_i}{1 + b_i p_i + b_j p_j} \right) \quad (9)$$

3- Governing transport models

A thorough understanding of gas transport in polymeric membranes is very important from industrial point of view. Moreover, designing new class of polymeric membranes requires a comprehensive knowledge of permeation mechanisms in the membrane. Accordingly, frame of reference/bulk flow model and Maxwell-Stefan were used as the two main models to investigate the transport and separation performance of propylene/propane binary mixture in polyimide membranes.

3-1- Frame of reference/bulk flow model

According to the frame of reference/bulk flow model, the transport of a binary gas mixture through the membrane can be presented as a ternary system comprised of two gases and a membrane using the following equations [40]:

$$n_1 = (n_1 + n_2 + n_m)w_1 - \rho D_{D1} \frac{dw_1}{dz} \quad (10)$$

$$n_2 = (n_1 + n_2 + n_m)w_2 - \rho D_{D2} \frac{dw_2}{dz} \quad (11)$$

$$n_m = (n_1 + n_2 + n_m)w_m - \rho D_{Dm} \frac{dw_m}{dz} \quad (12)$$

where n is the mass flux of components through the membrane and subscript m refers to the membrane. The first term of the right hand side is the convective or frame of reference term. This term is required to be considered when studying permeation in the membranes since diffusion of each molecule in a mixed gas environment is affected by the presence of other molecules which can produce an effective bulk flow [40, 42, 44].

Considering $n_m=0$, rearranging Eqs. (10) to (12) for flux of each component leads to the following equations:

$$n_1 = \frac{\rho D_{D1} \frac{dw_1}{dz}}{1 - (1 + 1/r)w_1} \quad (13)$$

$$n_2 = \frac{\rho D_{D2} \frac{dw_2}{dz}}{1 - (1 + r)w_2} \quad (14)$$

$$r = \frac{n_1}{n_2} \quad (15)$$

Boundary conditions are as follows:

$$z = 0; \quad p_1 = p_{1,0}; \quad p_2 = p_{2,0}; \quad w_1 = w_{1,0}; \quad w_2 = w_{2,0} \quad (16)$$

$$z = l; \quad p_1 = p_{1,l}; \quad p_2 = p_{2,l}; \quad w_1 = w_{1,l}; \quad w_2 = w_{2,l} \quad (17)$$

Mass fluxes of components 1 and 2 are obtained after integrating Eqs. (13) and (14) and applying the above boundary conditions [40]:

$$n_1 l = \frac{\rho D_{D1} \ln \frac{1-w_{1,l}(1+1/r)}{1-w_{1,0}(1+1/r)}}{1 + 1/r} \quad (18)$$

$$n_2 l = \frac{\rho D_{D2} \ln \frac{1-w_{2,l}(1+r)}{1-w_{2,0}(1+r)}}{1 + r} \quad (19)$$

Eqs. (18) and (19) should be solved for $n_1 l$ and $n_2 l$ iteratively in order to calculate the corresponding permeability using the following expression [44]:

$$P_1 = \frac{22400n_1l}{Mw_1\Delta p_1} \quad (20)$$

$$P_2 = \frac{22400n_2l}{Mw_2\Delta p_2} \quad (21)$$

Membrane selectivity can be calculated as follows [42]:

$$\alpha_{12} = \frac{P_1}{P_2} \quad (22)$$

3-2- Maxwell-Stefan model

In fact selection of a proper diffusion model in multi-component permeation is very crucial in modeling mixed gas transport. In most cases, the Fick's law is utilized assuming that the diffusion of each component is not affected by the presence of other components [46]. This assumption may not be true for permeation in some binary gas mixtures where the flux of one component can alter the diffusive and convective flux of the other component [40, 44].

The most common situation in which the Fick's law can fail to predict the mixed gas performance is when the diffusion coefficient of one component is affected by the diffusion of other components present in the mixture [46]. It means that D is a function of concentration which results to a more complex model [59-61]. Another situation is that the concentrations of the sorbed penetrants are not small in the polymer matrix. And the last situation is when the flux of one component is dependent on the gradient of concentration of other components [46]. Maxwell-Stefan model was presented as a logical starting framework to deal with the issue of coupling of fluxes [41, 46]. This model, which can be derived from kinetic theory, was developed originally to describe diffusion in gas mixtures and relates the forces acting on the

molecules of each species to the friction between these species and any other species [46, 48].

For a multi-component mixture Maxwell-Stefan equation can be written as follows [41, 46]:

$$d_i = - \sum_{j \neq i} \frac{x_i x_j}{D_{ij}} (v_i - v_j) \quad (23)$$

Where x and v are mole fraction and velocity, respectively. D_{ij} is the binary diffusion coefficient and d is driving force. Using mass fraction is more useful for describing diffusion in membrane systems [40, 46] as follows:

$$n_i = w_i \rho v_i \quad (24)$$

$$x_i = \frac{Mw}{Mw_i} w_i, \quad Mw = \left[\sum \frac{w_j}{Mw_j} \right]^{-1} \quad (25)$$

Using Eqs. (24) and (25) a more useful expression for describing mass transport in membranes can be obtained:

$$d_i = \sum_{j \neq i} \frac{Mw^2}{Mw_i Mw_j} \frac{n_i w_j - n_j w_i}{\rho D_{ij}} \quad (26)$$

Accordingly, for a system comprising two penetrants and a polymeric membrane the following equations are obtained:

$$d_1 = \frac{Mw^2}{Mw_1 Mw_2} \frac{n_1 w_2 - n_2 w_1}{\rho D_{12}} + \frac{Mw^2}{Mw_1 Mw_m} \frac{n_1 w_m}{\rho D_{1m}} \quad (27)$$

$$d_2 = \frac{Mw^2}{Mw_1 Mw_2} \frac{n_2 w_1 - n_1 w_2}{\rho D_{12}} + \frac{Mw^2}{Mw_2 Mw_m} \frac{n_2 w_m}{\rho D_{2m}} \quad (28)$$

The following redefinition of the diffusion coefficient leads to more simplified forms of the transport equations [41, 46].

$$D_{ij} = \mathcal{D}_{ij} \frac{Mw_j}{Mw} \quad (29)$$

Rearranging Eqs. (27) and (28) for the flux of each component, the Maxwell-Stefan equations reduce to:

$$d_1 = \left(\frac{Mw}{Mw_2} \frac{w_2}{\rho D_{12}} + \frac{Mw}{Mw_m} \frac{w_m}{\rho D_{1m}} \right) n_1 - \frac{Mw}{Mw_2} \frac{w_1}{\rho D_{12}} n_2 \quad (30)$$

$$d_2 = \left(\frac{Mw}{Mw_1} \frac{w_1}{\rho D_{12}} + \frac{Mw}{Mw_m} \frac{w_m}{\rho D_{2m}} \right) n_2 - \frac{Mw}{Mw_1} \frac{w_2}{\rho D_{12}} n_1 \quad (31)$$

The driving force can be defined via the following expression [46]:

$$C_{md} RT d_i = C_i \frac{d\mu_i}{dz} - w_i \frac{dp_m}{dz} \quad (32)$$

Where C_{md} and C are the molar density of the mixture and the molar concentration and p_m is the pressure in the membrane. Chemical potential, μ , is defined as follows:

$$\frac{d\mu_i}{dz} = RT \frac{d \ln a_i}{dz} + \bar{v}_i \frac{dp_m}{dz} \quad (33)$$

Where a is the activity defined as the ratio of partial fugacity to the standard fugacity. The latter is taken always as that of unity so the activity is numerically the same as the partial fugacity. By assuming the ideal gas law, partial fugacity can be represented by partial pressure. Since the pressure throughout the membrane is constant therefore: $dp_m/dz=0$ [46]. Accordingly, driving force can be written as follows:

$$d_i = \frac{Mw}{Mw_i} w_i \frac{d \ln p_i}{dz} \quad (34)$$

It can be rewritten in the following form:

$$d_i = \frac{Mw}{Mw_i} \frac{C_i}{p_i} \frac{dp_i}{dC_i} \frac{dw_i}{dz} \quad (35)$$

Substituting Eq. (35) in Eqs. (30) and (31) the following equations can be obtained:

$$\rho \frac{C_1}{p_1} \frac{dp_1}{dC_1} \frac{dw_1}{dz} = \left(\varepsilon_1 \frac{w_2}{D_{1m}} + \frac{w_m}{D_{1m}} \right) n_1 - \varepsilon_1 \frac{w_1}{D_{1m}} n_2 \quad (36)$$

$$\rho \frac{C_2}{p_2} \frac{dp_2}{dC_2} \frac{dw_2}{dz} = \left(\varepsilon_2 \frac{w_1}{D_{2m}} + \frac{w_m}{D_{2m}} \right) n_2 - \varepsilon_2 \frac{w_2}{D_{2m}} n_1 \quad (37)$$

$$\varepsilon_1 = \frac{D_{1m}}{D_{12}}, \quad \varepsilon_2 = \frac{Mw_2}{Mw_1} \frac{D_{2m}}{D_{12}} \quad (38)$$

where ε_1 and ε_2 are frictional coupling effects [41].

Eqs. (36) and (37) can be written in the matrix form as follows:

$$n = -\rho B \eta^{-1} \nabla w \quad (39)$$

This allows evaluating the contribution of kinetic coupling effects, B , and thermodynamic coupling effects (TCE), η , independently. The matrices are provided in Eqs. (40) and (41):

$$B = \begin{bmatrix} \varepsilon_1 \frac{w_2}{D_{1m}} + \frac{w_m}{D_{1m}} & -\varepsilon_1 \frac{w_1}{D_{1m}} \\ -\varepsilon_2 \frac{w_2}{D_{2m}} & \varepsilon_2 \frac{w_1}{D_{2m}} + \frac{w_m}{D_{2m}} \end{bmatrix} \quad (40)$$

and

$$\eta = \begin{bmatrix} \eta_{11} & \eta_{12} \\ \eta_{21} & \eta_{22} \end{bmatrix} = \begin{bmatrix} \frac{C_1 dp_1}{p_1 dC_1} & \frac{C_1 dp_1}{p_1 dC_2} \\ \frac{C_2 dp_2}{p_2 dC_1} & \frac{C_2 dp_2}{p_2 dC_2} \end{bmatrix} \quad (41)$$

The off-diagonal elements of the matrix η are indicators of the thermodynamic coupling of fluxes [62]. The term dp_i/dC_j should be calculated in order to calculate the elements of η . For instance, η_{ij} is defined as the degree of influence of flux of component j on the flux of component i in the mixture. After considerable algebraic operations, the following equations are obtained by simultaneous solving of sorption equations (i.e., Eq. (3)) for components 1 and 2.

$E_1 p_1^3 + F_1 p_1^2 + G_1 p_1 + H_1 = 0$	(42)
$E_2 p_2^3 + F_2 p_2^2 + G_2 p_2 + H_2 = 0$	(43)

Where coefficients E , F , G and H are provided in Table 1.

Elements of thermodynamic matrix can be calculated by differentiation of Eqs. (42) and (43) with respect to concentration (C).

Accordingly, the elements of TCE matrix can be obtained as follows:

$\eta_{11} = -\frac{C_1}{p_1} \left(\frac{\frac{dE_1}{dC_1} p_1^3 + \frac{dF_1}{dC_1} p_1^2 + \frac{dG_1}{dC_1} p_1 + \frac{dH_1}{dC_1}}{3p_1^2 E_1 + 2p_1 F_1 + G_1} \right)$	(44)
$\eta_{12} = -\frac{C_1}{p_1} \left(\frac{\frac{dE_1}{dC_2} p_1^3 + \frac{dF_1}{dC_2} p_1^2 + \frac{dG_1}{dC_2} p_1 + \frac{dH_1}{dC_2}}{3p_1^2 E_1 + 2p_1 F_1 + G_1} \right)$	(45)
$\eta_{21} = -\frac{C_2}{p_2} \left(\frac{\frac{dE_2}{dC_1} p_2^3 + \frac{dF_2}{dC_1} p_2^2 + \frac{dG_2}{dC_1} p_2 + \frac{dH_2}{dC_1}}{3p_2^2 E_2 + 2p_2 F_2 + G_2} \right)$	(46)
$\eta_{22} = -\frac{C_2}{p_2} \left(\frac{\frac{dE_2}{dC_2} p_2^3 + \frac{dF_2}{dC_2} p_2^2 + \frac{dG_2}{dC_2} p_2 + \frac{dH_2}{dC_2}}{3p_2^2 E_2 + 2p_2 F_2 + G_2} \right)$	(47)

Where the gradients dE_i/dC_j , dF_i/dC_j , dG_i/dC_j and dH_i/dC_j are provided in Table 2.

4- Results and discussion

The development of advanced polymeric membranes for propylene/propane separation requires a thorough understanding about the factors affecting the transport of penetrants within the membrane. Therefore, it is important to adopt a proper approach in order to predict the performance of the membrane mathematically. Both frame of reference/bulk flow and Maxwell-Stefan models allow accounting for the coexistence of the penetrating molecules through the membrane and hence the results may be helpful to examine the commercial viability of the polyimides. On the other hand, Maxwell-Stefan model originally accounts for the coupling of fluxes of two penetrants while frame of reference/bulk flow model does not. According to the Maxwell-Stefan model, the flux of one component is dependent on the gradient of concentration

of other component in a binary mixture while this issue was not considered in the Fick's law which is the foundation of the frame of reference/bulk flow model. Moreover, matrix form of Maxwell-Stefan model can be employed to assess the contributions of kinetic and thermodynamic coupling effects independently. In the present study, sorption data of pure propylene and propane in 6FDA-6FpDA [44, 45], 6FDA-DAM [43] and 6FDA-TrMPD [36] were used to predict the separation performance of membrane in the case of equimolar (50/50) binary gas mixture. These data are presented in Table 3.

4-1- Analysis of sorption for pure and binary gas mixture

Sorption in glassy polymers can be well described using dual mode sorption in the base case. This model describes the sorption using the assumption that two regimes are responsible for the penetrant sorption. One regime is the unrelaxed free volume of the glassy polymer and sorption into these sites can be described by the Langmuir model. The other regime is the sorption in densified polymer chains responsible for Henry's law domains that dominates at high pressures when free volume becomes saturated [40, 43].

Fig. 1 shows the sorption values as a function of pressure using dual mode sorption model calculated based on sorption data of pure gases. It is evident that considering pure components, sorption of propylene is higher than that of propane in all polyimides indicating higher solubility of propylene than that of propane. According to the data in Table 3, this can mainly be owing to the larger Langmuir capacity constant (C'_H) of the polymers for propylene than propane, indicating the dominating role of Langmuir sites in the sorption process. Interestingly, a limited difference between the sorption of propylene and propane was observed in case of 6FDA-TrMPD (Fig. 1 (d)) compared to the rest of polyimides. It was also noted that, sorption values for

propylene and propane in the binary gas mixture were lower than those of respective pure components. This can be attributed to the contribution of additional $b_j p_j$ term in the denominator of Langmuir component provided in Eq. 5. In addition, results reveal a generally more pronounced drop in the sorption of propylene when coexists with propane in a binary gas mixture. Larger drops observed for 6FDA-DAM and 6FDA-TrMPD (Fig. 1 (c) and (d)) compared to other polyimides can be attributed to the dominating role of Langmuir affinity constants in these polymers for Propane. Therefore, the larger decrease in the sorption of the faster component in the binary gas mixture can be attributed to the competition effect and/or contribution of bulk flow that are not taken into account in dual mode sorption model [40, 44].

Fig. 2 demonstrates the corresponding values of sorption level for the investigated polymers. A similar trend of higher sorption level of propylene than that of propane can be seen for all polymers except for 6FDA-TrMPD in pure state. This can be attributed to the larger Henry constant (k_D) of propane compared to that of propylene in 6FDA-TrMPD (Table 3) compared to other polymers.

In addition, sorption levels for propylene and propane in the binary gas mixture were lower than those of respective pure components as explained earlier. The exceptionally lower sorption level of propylene in binary gas mixture than that of propane in 6FDA-TrMPD can be explained by data presented in Fig. 3 indicating a larger sorption level of propane in Henry sites (W_{D2}) arising from the larger contribution of Henry constants of 6FDA-TrMPD for this gas.

Moreover, sorption level of propane in 6FDA-TrMPD is the highest among other polyimides due to the highest k_D and bC'_H while sorption level of propylene is higher in 6FDA-6FpDA at 35 °C despite lower values of k_D and bC'_H compared to that of 6FDA-TrMPD. Sorption levels for propylene and propane are presented in Fig. 4.

The highest values of propylene sorption level in 6FDA-6FpDA at 35 °C compared to other polyimides can arise from its highest value of F among other polyimides (Table 3). In order to prove this hypothesis, mobile fraction of Langmuir population in all the studied polyimides were depicted (Fig. 5) and it was observed that this value in 6FDA-6FpDA at 35 °C is the highest among other polyimides. In other words, mobile fraction of Langmuir population play an important role in determining the sorption level even in the case of small values for k_D and bC'_H .

4-2- Analysis of frame of reference/bulk flow model

According to the frame of reference/bulk flow model, the transport process is considered as a combination of both bulk and diffusive fluxes. Bulk flux is a function of sorption level in permeation of pure components; however in the case of binary gas mixtures, bulk flux is a function of both sorption level and flux of mobile components [40]. The contributions of bulk flux of propylene and propane in different polyimides were calculated according to the method described by Kamaruddin and Koros [40] and are presented in Fig. 6.

It can be observed that the flux of propane in the binary mixture of propylene/propane is much higher than that of pure propane while the flux of propylene remained almost unchanged. It can be inferred that propane molecules swept by the faster penetrant, propylene, and this led to an effective bulk flow of propane.

In addition, Fig. 7 shows that the contribution of bulk flux for propane is much higher in the 6FDA-TrMPD compared to other polyimides. This may be due to the higher sorption level of propane in this polymer as illustrated in Fig. 4 (b).

It is obvious that bulk flux of propane, which was not accounted for in the dual mode model, constitute a great portion of the total mass flux. This consideration led to more accurate predictions of the separation performance in the case of 6FDA-6FpDA. Nevertheless, this model failed to predict permeability and selectivity in 6FDA-DAM and 6FDA-TrMPD. Even more, applying this model led to the wrong predictions for the trend of selectivity in the case of 6FDA-DAM. This may be attributed to the fact that the flux of each component is dependent on the gradient of concentration of other component as explained by Paul [46] and can be accounted for by the Maxwell-Stefan model. It should also be noted that different testing temperatures as well as the chemical structure of the studied polymers may paly parts in the obtained trends.

4-3- Analysis of Maxwell-Stefan model

According to Maxwell-Stefan model the flux of each component is related to the driving force of both components. In fact, driving force is a combination of the material fluxes which in turn can be expressed in terms of composition gradients [49, 63]. Accordingly, coupling of fluxes is inherently accounted for in this model which was not considered in the bulk flow model.

Propylene/propane selectivity for 6FDA-6FpDA at different upstream pressures calculated using both frame of reference/bulk flow and Maxwell-Stefan models is presented in Fig. 8. It can be observed that predictions of both models are in agreement with the experimental data of permeation in binary gas mixture presented by Das and Koros [44]. In addition, predicted values of the frame of reference/bulk flow model are almost the same as those calculated by the Maxwell-Stefan model. This can be due to the negligible cross-terms of the kinetic coupling matrix resulted from the infinite small values of frictional coupling effects. This in turn arises from markedly small values of diffusion coefficients of penetrants, D_{1m} and D_{2m} , compared to the

coupling diffusion coefficient, D_{12} . Experimental dual mode diffusion coefficients (provided in Table 3) were used as D_{1m} and D_{2m} and D_{12} were calculated according to the Chapman-Enskog Wilke-Lee model [64].

Besides, the weight fractions of the sorbed species in the polymer matrix are small enough to assume $w_m \approx 1$. The average values of frictional coupling effects (ε_1 and ε_2), sorption level in membrane (w_m) and the calculated kinetic coupling effects ($B_{average}$) are listed in Table 4. Consequently, predictions of Maxwell-Stefan model approached to that of bulk flow model which can also be observed in Figs. 9 and 10.

Due to the nature of the propane and propylene which are often separated at relatively low pressures and high temperatures (i.e. at low activities), the observed effect of pressure on selectivity (Fig. 8) and permeability (Figs. 9 and 10) in this case is quite modest. More pronounced effects are expected for other gas pairs permeating at higher pressures and is the subject of our ongoing investigations.

However, it was found that the predictions of the aforementioned models deviated from experimental data in Figs. 9 and 10 reported respectively by Burns and Koros [43] and Tanaka et al. [36] in the case of propane permeability. Whereas, Maxwell-Stefan model with TCE contribution led to a better estimation of permeability of propane according to Figs. 9 and 10.

Comparison of the data related to the TCE matrix presented in Fig. 11, reveals that the cross terms are not negligible versus the main terms suggesting that the diffusive fluxes of propane and propylene are affected to some extent when present in the mixture. On the other hand, higher values of η_{12} compared to η_{21} may suggest that diffusive flux of propylene is strongly coupled with that of propane. This can be a justifiable reason for less accurate prediction of permeability of propane than that of propylene by Maxwell-Stefan model without TCE contribution.

Therefore, the assumption that the gradient of concentration of each component can affect the flux of other component seems to be valid when studying the transport of propylene/propane binary mixture through polyimide membranes. The average values of thermodynamic coupling effects are presented in Table 5.

Despite the importance of TCEs and their effective role in providing a better estimation of the transport behavior in the mentioned systems, it is obvious that TCEs could not be the only decisive parameters in determining the transport properties of binary gas mixture. As it was mentioned before, sorption data of pure gases were used to estimate the behavior of binary gas mixture while it was proved that the presence of penetrants in the binary gas mixture led to an effective bulk flow for each component. Accordingly, it can be speculated that diffusion of each component can also be affected in their binary gas mixture. This was investigated by calculating the diffusion coefficients using experimental permeability and selectivity of binary gas mixture employing Maxwell-Stefan model both without and with contribution of TCEs. The calculated values are presented in Table 4 and used for analysis of the separation performance of 6FDA-DAM and 6FDA-TrMPD. Comparing the calculated diffusion coefficients and the diffusion coefficients of pure gases in Table 6 it can be observed that the optimized diffusion coefficients of propylene in the binary gas system in both 6FDA-DAM and 6FDA-TrMPD reduced to almost half of their original values. However, the optimized diffusion coefficient of propane stayed almost unchanged in 6FDA-DAM while increased in 6FDA-TrMPD.

The reduced diffusion coefficient of propylene could be ascribed to the competitive sorption of propane and propylene in the binary gas mixture. In addition, using the results illustrated in Fig. 11, it can be inferred that the flux of larger molecule, propane, probably hindered propylene molecules to diffuse unlike the case of pure gas. This phenomenon did not disturb the diffusion

of propane in the binary gas environment through 6FDA-DAM. Therefore, another phenomenon might act to increase the diffusion coefficient of propane in 6FDA-TrMPD. According to Fig. 2 (d), propane sorption level is higher than that of propylene both in pure and binary gas systems which makes the polyimide susceptible to plasticization. Therefore, one probable reason for the increase in the propane diffusion coefficient in the case of 6FDA-TrMPD could be the plasticization phenomena. The trend in the permeability of propane could be also a clue to the presence of this phenomena in the mentioned polyimide since a minimum permeability can be observed in Fig. 10.

Figs. 12 and 13 show the separation performance of both 6FDA-DAM [43] and 6FDA-TrMPD [36] predicted by Maxwell-Stefan model without and with TCE contribution using data in Table 4. These figures indicate that diffusion coefficients that obtained via performing optimization using the Maxwell-Stefan model with TCE contribution resulted in better estimation of separation performance compared to the Maxwell-Stefan model in which TCEs were not taken into account. The optimized diffusion coefficients can also be used to estimate the propylene/propane separation performance of the polyimides in pressures other than those used for the optimization.

5- Conclusions

Transport of propylene and propane through polyimide membranes were investigated and analyzed by applying two major phenomenological models of frame of reference/bulk flow and Maxwell-Stefan. Results revealed that sorption level of the more soluble gas, propylene, calculated using the dual sorption model, was generally higher than that of propane and is highly affected by the values of k_D , bC'_H and F . Frame of reference/bulk flow model led to good

estimations of the membrane performance in the case of 6FDA-6FpDA while could not provide appropriate predictions for the separation performance of binary gas mixture in the case of 6FDA-DAM and 6FDA-TrMPD. This was attributed to the dependence of the flux of each component to the gradient of concentration of other component. The validity of this speculation was assessed via applying the Maxwell-Stefan model that initially accounted for the co-existence of penetrants. According to the results, Maxwell-Stefan estimations approached to those of frame of reference/bulk flow model due to the small values of the cross terms in the matrix of the kinetic coupling effects. Better predictions were obtained using Maxwell-Stefan model with TCE contribution. Calculating optimized diffusion coefficients by the aid of experimental permeability showed that diffusion coefficients were also affected due to the presence of another component in the binary gas mixture. Diffusion coefficients of all components decreased in the binary gas mixture while that of propane in 6FDA-TrMPD increased. This could be probably due to the plasticization phenomena since the sorption level of propane in 6FDA-TrMPD was higher compared to other polyimides. In addition, the optimized diffusion coefficients could be utilized to predict the behavior of propylene/propane separation in other pressures than those used for the optimization. The findings can be effectively used by researchers for selecting the best strategies in order to represent the best possible predictions about the membrane separation performance for olefin/paraffin separation applications. Nevertheless, more investigations are required to reach to more reliable conclusions which necessitate more experimentations and analysis.

Nomenclature

<i>a</i>	activity
<i>b</i>	Langmuir affinity constant [1/psia]

B	matrix of kinetic coupling effects
C	gas sorption [cm^3 (STP)/ cm^3 (polymer)]
C_D	concentration of Henry's law sites [cm^3 (STP)/ cm^3 (polymer)]
C_H	concentration of Langmuir sites [cm^3 (STP)/ cm^3 (polymer)]
C'_H	Langmuir capacity constant [cm^3 (STP)/ cm^3 (polymer)]
d	driving force
D_D	diffusion coefficient in the Henry's law environment [m^2/s]
D_H	diffusion coefficient in the Langmuir domain [m^2/s]
D_{ij}	binary diffusion coefficient [m^2/s]
J	molar flux through membrane [cm^3 (STP)/ cm^2 s]
k_D	Henry's law constant [cm^3 (STP)/ cm^3 (polymer) psia]
l	membrane thickness [m]
M_w	molecular weight [g/mol]
n	trans membrane mass flux [$\text{kg}/\text{s m}^2$]
p	pressure [psia]
P	permeability [Barrer]=[cm^3 (STP) cm/cm^2 s cmHg]
r	ratio of mass flux of propylene to the mass flux of propane
R	universal gas constant [J/mol. K]
T	temperature [K]
w	sorption level (g/g)
w_D	sorption level in Henry's law sites (g/g)
w_H	sorption level in Langmuir sites (g/g)
x	mole fraction
z	membrane length coordinate [m]
<i>Greek letters</i>	
α	membrane selectivity
ε	frictional coupling effects
η	matrix of thermodynamic coupling effects
μ	chemical potential [J/mole]

v	velocity [m/s]
ρ	average density of the polymer [kg/m ³]

Subscripts

i, j	Index of components
ij	interaction of component i and j
m	membrane
0	upstream side of the membrane
l	downstream side of the membrane
1	Propylene
2	Propane

References

- [1] Y. Yampolskii, Polymeric Gas Separation Membranes, *Macromolecules*, 45 (2012) 3298-3311.
- [2] P. Bernardo, E. Drioli, Membrane gas separation progresses for process intensification strategy in the petrochemical industry, *Pet. Chem.*, 50 (2010) 271-282.
- [3] C.A. Scholes, G.W. Stevens, S.E. Kentish, Membrane gas separation applications in natural gas processing, *Fuel*, 96 (2012) 15-28.
- [4] R.W. Baker, Future Directions of Membrane Gas Separation Technology, *Industrial & Engineering Chemistry Research*, 41 (2002) 1393-1411.
- [5] R.W. Baker, Membrane Technology in the Chemical Industry: Future Directions, in: *Membrane Technology*, Wiley-VCH Verlag GmbH & Co. KGaA, 2006, pp. 305-335.
- [6] H. Bum Park, E.M.V. Hoek, V.V. Tarabara, Gas Separation Membranes, in: *Encyclopedia of Membrane Science and Technology*, John Wiley & Sons, Inc., 2013.
- [7] S.S. Hosseini, M.M. Teoh, T.S. Chung, Hydrogen separation and purification in membranes of miscible polymer blends with interpenetration networks, *Polymer*, 49 (2008) 1594-1603.
- [8] S.S. Hosseini, Y. Li, T.-S. Chung, Y. Liu, Enhanced gas separation performance of nanocomposite membranes using MgO nanoparticles, *Journal of Membrane Science*, 302 (2007) 207-217.
- [9] N.W. Ockwig, T.M. Nenoff, Membranes for Hydrogen Separation, *Chemical Reviews*, 107 (2007) 4078-4110.
- [10] S.S. Hosseini, T.S. Chung, Carbon membranes from blends of PBI and polyimides for N₂/CH₄ and CO₂/CH₄ separation and hydrogen purification, *Journal of Membrane Science*, 328 (2009) 174-185.
- [11] S.S. Hosseini, N. Peng, T.S. Chung, Gas separation membranes developed through integration of polymer blending and dual-layer hollow fiber spinning process for hydrogen and natural gas enrichments, *Journal of Membrane Science*, 349 (2010) 156-166.
- [12] Y. Xiao, B.T. Low, S.S. Hosseini, T.S. Chung, D.R. Paul, The strategies of molecular architecture and modification of polyimide-based membranes for CO₂ removal from natural gas—A review, *Progress in Polymer Science*, 34 (2009) 561-580.
- [13] S.I. Semenova, Polymer membranes for hydrocarbon separation and removal, *Journal of Membrane Science*, 231 (2004) 189-207.

- [14] Y. Yampolskii, L. Starannikova, N. Belov, M. Bermeshev, M. Gringolts, E. Finkelshtein, Solubility controlled permeation of hydrocarbons: New membrane materials and results, *Journal of Membrane Science*, 453 (2014) 532-545.
- [15] S.S. Hosseini, S.M. Roodashti, P.K. Kundu, N.R. Tan, Transport properties of asymmetric hollow fiber membrane permeators for practical applications: Mathematical modeling for binary gas mixtures *Canadian journal of chemical engineering*, In Press (2014).
- [16] R. Faiz, K. Li, Polymeric membranes for light olefin/paraffin separation, *Desalination*, 287 (2012) 82-97.
- [17] R. Faiz, K. Li, Olefin/paraffin separation using membrane based facilitated transport/chemical absorption techniques, *Chemical Engineering Science*, 73 (2012) 261-284.
- [18] R.L. Burns, W.J. Koros, Defining the challenges for C_3H_6/C_3H_8 separation using polymeric membranes, *Journal of Membrane Science*, 211 (2003) 299-309.
- [19] S. Bai, S. Sridhar, A.A. Khan, Recovery of propylene from refinery off-gas using metal incorporated ethylcellulose membranes, *Journal of Membrane Science*, 174 (2000) 67-79.
- [20] M. Rungta, C. Zhang, W.J. Koros, L. Xu, Membrane-based ethylene/ethane separation: The upper bound and beyond, *AIChE Journal*, 59 (2013) 3475-3489.
- [21] J. Ploegmakers, A.R.T. Jelsma, A.G.J. van der Ham, K. Nijmeijer, Economic Evaluation of Membrane Potential for Ethylene/Ethane Separation in a Retrofitted Hybrid Membrane-Distillation Plant Using Unisim Design, *Industrial & Engineering Chemistry Research*, 52 (2013) 6524-6539.
- [22] M.S. Avgidou, S.P. Kaldis, G.P. Sakellariopoulos, Membrane cascade schemes for the separation of LPG olefins and paraffins, *Journal of Membrane Science*, 233 (2004) 21-37.
- [23] V. Pirouzfard, S.S. Hosseini, M.R. Omidkhah, A.Z. Moghaddam, Modeling and optimization of gas transport characteristics of carbon molecular sieve membranes through statistical analysis, *Polymer Engineering & Science*, 54 (2013) 147-157.
- [24] V. Pirouzfard, A.Z. Moghaddam, M.R. Omidkhah, S.S. Hosseini, Investigating the effect of dianhydride type and pyrolysis condition on the gas separation performance of membranes derived from blended polyimides through statistical analysis, *Journal of Industrial and Engineering Chemistry*, 20 (2013) 1061-1070.
- [25] S.S. Hosseini, M.R. Omidkhah, A. Zarringhalam Moghaddam, V. Pirouzfard, W.B. Krantz, N.R. Tan, Enhancing the properties and gas separation performance of PBI-polyimides blend carbon molecular sieve membranes via optimization of the pyrolysis process, *Separation and Purification Technology*, 122 (2014) 278-289.
- [26] M. Askari, T.-S. Chung, Natural gas purification and olefin/paraffin separation using thermal cross-linkable co-polyimide/ZIF-8 mixed matrix membranes, *Journal of Membrane Science*, 444 (2013) 173-183.
- [27] M. Askari, Y. Xiao, P. Li, T.-S. Chung, Natural gas purification and olefin/paraffin separation using cross-linkable 6FDA-Durene/DABA co-polyimides grafted with α , β , and γ -cyclodextrin, *Journal of Membrane Science*, 390-391 (2012) 141-151.
- [28] J.J. Krol, M. Boerrigter, G.H. Koops, Polyimide hollow fiber gas separation membranes: preparation and the suppression of plasticization in propane/propylene environments, *Journal of Membrane Science*, 184 (2001) 275-286.
- [29] T. Visser, M. Wessling, Auto and mutual plasticization in single and mixed gas C_3 transport through Matrimid-based hollow fiber membranes, *Journal of Membrane Science*, 312 (2008) 84-96.
- [30] S.S. Chan, R. Wang, T.-S. Chung, Y. Liu, C_2 and C_3 hydrocarbon separations in poly(1,5-naphthalene-2,2'-bis(3,4-phthalic) hexafluoropropane) diimide (6FDA-1,5-NDA) dense membranes, *Journal of Membrane Science*, 210 (2002) 55-64.
- [31] C. Staudt-Bickel, W.J. Koros, Olefin/paraffin gas separations with 6FDA-based polyimide membranes, *Journal of Membrane Science*, 170 (2000) 205-214.
- [32] M. Yoshino, S. Nakamura, H. Kita, K.-i. Okamoto, N. Tanihara, Y. Kusuki, Olefin/paraffin separation performance of asymmetric hollow fiber membrane of 6FDA/BPDA-DDBT copolyimide, *Journal of Membrane Science*, 212 (2003) 13-27.

- [33] Y. Tsujita, Gas sorption and permeation of glassy polymers with microvoids, *Progress in Polymer Science*, 28 (2003) 1377-1401.
- [34] W.J. Koros, Model for sorption of mixed gases in glassy polymers, *Journal of Polymer Science: Polymer Physics Edition*, 18 (1980) 981-992.
- [35] D.R. Paul, W.J. Koros, Effect of partially immobilizing sorption on permeability and the diffusion time lag, *Journal of Polymer Science: Polymer Physics Edition*, 14 (1976) 675-685.
- [36] K. Tanaka, A. Taguchi, J. Hao, H. Kita, K. Okamoto, Permeation and separation properties of polyimide membranes to olefins and paraffins, *Journal of Membrane Science*, 121 (1996) 197-207.
- [37] W.J. Koros, D.R. Paul, A.A. Rocha, Carbon dioxide sorption and transport in polycarbonate, *Journal of Polymer Science: Polymer Physics Edition*, 14 (1976) 687-702.
- [38] M. Askari, M.L. Chua, T.-S. Chung, Permeability, Solubility, Diffusivity, and PALS Data of Cross-linkable 6FDA-based Copolyimides, *Industrial & Engineering Chemistry Research*, 53 (2014) 2449-2460.
- [39] O.C. David, D. Gorri, A. Urriaga, I. Ortiz, Mixed gas separation study for the hydrogen recovery from H₂/CO/N₂/CO₂ post combustion mixtures using a Matrimid membrane, *Journal of Membrane Science*, 378 (2011) 359-368.
- [40] D.H. Kamaruddin, W.J. Koros, Some observations about the application of Fick's first law for membrane separation of multicomponent mixtures, *Journal of Membrane Science*, 135 (1997) 147-159.
- [41] D.R. Paul, Reformulation of the solution-diffusion theory of reverse osmosis, *Journal of Membrane Science*, 241 (2004) 371-386.
- [42] M.J. Thundiyil, Y.H. Jois, W.J. Koros, Effect of permeate pressure on the mixed gas permeation of carbon dioxide and methane in a glassy polyimide, *Journal of Membrane Science*, 152 (1999) 29-40.
- [43] R.L. Burns, Investigation of poly(pyrrolone-imide) materials for the olefin / paraffin separation in: *Chemical Engineering Department, University of Texas at Austin*, 2002, pp. 232.
- [44] M. Das, W.J. Koros, Performance of 6FDA-6FpDA polyimide for propylene/propane separations, *Journal of Membrane Science*, 365 (2010) 399-408.
- [45] M. Das, Membranes for olefin/paraffin separation, in: *Chemical engineering, Georgia institute of technology*, 2009, pp. 206.
- [46] D.R. Paul, 1.04 - Fundamentals of transport phenomena in polymer membranes, in: E. Drioli, L. Giorno (Eds.) *Comprehensive membrane science and engineering*, Elsevier, Oxford, 2010, pp. 75-90.
- [47] R.D. Raharjo, B.D. Freeman, D.R. Paul, G.C. Sarti, E.S. Sanders, Pure and mixed gas CH₄ and n-C₄H₁₀ permeability and diffusivity in poly(dimethylsiloxane), *Journal of Membrane Science*, 306 (2007) 75-92.
- [48] J. Bausa, W. Marquardt, Detailed modeling of stationary and transient mass transfer across pervaporation membranes, *AIChE Journal*, 47 (2001) 1318-1332.
- [49] F. Fornasiero, J.M. Prausnitz, C.J. Radke, Multicomponent Diffusion in Highly Asymmetric Systems. An Extended Maxwell-Stefan Model for Starkly Different-Sized, Segment-Accessible Chain Molecules, *Macromolecules*, 38 (2005) 1364-1370.
- [50] A.A. Ghoreyshi, F.A. Farhadpour, M. Soltanieh, A general model for multicomponent transport in nonporous membranes based on maxwell-stefan formulation, *Chemical Engineering Communications*, 191 (2004) 460-499.
- [51] F. Kapteijn, W.J.W. Bakker, G. Zheng, J. Poppe, J.A. Moulijn, Permeation and separation of light hydrocarbons through a silicalite-1 membrane: Application of the generalized Maxwell-Stefan equations, *The Chemical Engineering Journal and the Biochemical Engineering Journal*, 57 (1995) 145-153.
- [52] P.J.A.M. Kerkhof, A modified Maxwell-Stefan model for transport through inert membranes: the binary friction model, *The Chemical Engineering Journal and the Biochemical Engineering Journal*, 64 (1996) 319-343.
- [53] C.P. Ribeiro Jr, B.D. Freeman, D.R. Paul, Modeling of multicomponent mass transfer across polymer films using a thermodynamically consistent formulation of the Maxwell-Stefan equations in terms of volume fractions, *Polymer*, 52 (2011) 3970-3983.

- [54] S. Najari, S.S. Hosseini, N.R. Tan, Analysis of the transport models governing permeation and separation of olefin/paraffin mixtures in polymeric membranes, in: 9th Ibero-American Conference on Membrane Science and Technology (CITEM 2014), Santander, Spain, 2014.
- [55] D.R. Paul, Gas Sorption and Transport in Glassy Polymers, *Berichte der Bunsengesellschaft für physikalische Chemie*, 83 (1979) 294-302.
- [56] W. Koros, D. Punsalan, Polymer glasses: Diffusion in, in: Editors-in-Chief., K.H.J. Buschow, W.C. Robert, C.F. Merton, I. Bernard, J.K. Edward, M. Subhash, V. Patrick (Eds.) *Encyclopedia of Materials: Science and Technology* (Second Edition), Elsevier, Oxford, 2001, pp. 7305-7315.
- [57] W.J. Koros, R.T. Chern, V. Stannett, H.B. Hopfenberg, A model for permeation of mixed gases and vapors in glassy polymers, *Journal of Polymer Science: Polymer Physics Edition*, 19 (1981) 1513-1530.
- [58] G. Park, Transport Principles—Solution, Diffusion and Permeation in Polymer Membranes, in: P.M. Bungay, H.K. Lonsdale, M.N. Pinho (Eds.) *Synthetic Membranes: Science, Engineering and Applications*, Springer Netherlands, 1986, pp. 57-107.
- [59] J.H. Petropoulos, Quantitative analysis of gaseous diffusion in glassy polymers, *Journal of Polymer Science Part A-2: Polymer Physics*, 8 (1970) 1797-1801.
- [60] S.A. Stern, V. Saxena, Concentration-dependent transport of gases and vapors in glassy polymers, *Journal of Membrane Science*, 7 (1980) 47-59.
- [61] M. Klopffer, H., B. Flaconnèche, Transport de molécules gazeuses dans les polymères: revue bibliographique, *Oil & Gas Science and Technology - Rev. IFP*, 56 (2001) 223-244.
- [62] A.A. Ghoreyshi, F.A. Farhadpour, M. Soltanieh, M. Abdelghani, Transport of small polar molecules across nonporous polymeric membranes: II. Shortcomings of phenomenological models of membrane transport, *Journal of Membrane Science*, 211 (2003) 215-234.
- [63] S.A.A. Ghoreyshi, F.A. Farhadpour, M. Soltanieh, Multicomponent transport across nonporous polymeric membranes, *Desalination*, 144 (2002) 93-101.
- [64] R.E. Treybal, *Mass-transfer Operations*, McGraw-Hill, 1988.

Table 1. Equations derived from sorption equations and their respective coefficients.

$E_1 p_1^3 + F_1 p_1^2 + G_1 p_1 + H_1 = 0$	$E_2 p_2^3 + F_2 p_2^2 + G_2 p_2 + H_2 = 0$
$E_1 = k_{D1} k_{D2} b_1^2 b_2 C_{H1} - k_{D1}^2 b_1 b_2^2 C_{H2}$	$E_2 = k_{D1} k_{D2} b_2^2 b_1 C_{H2} - k_{D2}^2 b_2 b_1^2 C_{H1}$
$F_1 = 2k_{D1} b_1 b_2^2 C_1 C_{H2} - k_{D1}^2 b_2^2 C_{H2} - k_{D1} b_1 b_2^2 C_{H1} C_{H2}$ $+ k_{D1} b_1 b_2^2 C_2 C_{H2} + k_{D2} b_1^2 b_2 C_{H1}^2$ $+ k_{D1} k_2 b_1 b_2 C_{H1} - k_{D2} b_1^2 b_2 C_1 C_{H1}$	$F_2 = 2k_{D2} b_2 b_1^2 C_2 C_{H1} - k_{D2}^2 b_1^2 C_{H1} - k_{D2} b_2 b_1^2 C_{H1} C_{H2}$ $+ k_{D2} b_2 b_1^2 C_1 C_{H1} + k_{D1} b_2^2 b_1 C_{H2}^2$ $+ k_{D1} k_{D2} b_1 b_2 C_{H2} - k_{D1} b_2^2 b_1 C_2 C_{H2}$
$G_1 = 2k_{D1} b_2^2 C_1 C_{H2} + b_1 b_2^2 C_1 C_{H1} C_{H2} - b_1 b_2^2 C_1 C_2 C_{H1}$ $- b_1 b_2^2 C_1^2 C_{H2} - k_{D2} b_1 b_2 C_1 C_{H1}$	$G_2 = 2k_{D2} b_1^2 C_2 C_{H1} + b_2 b_1^2 C_2 C_{H1} C_{H2} - b_2 b_1^2 C_1 C_2 C_{H2}$ $- b_2 b_1^2 C_2^2 C_{H1} - k_{D1} b_1 b_2 C_2 C_{H2}$
$H_1 = -b_2^2 C_1^2 C_{H2}$	$H_2 = -b_1^2 C_2^2 C_{H1}$

Table 2. The elements of TCE matrix and their respective gradients.

η_{11}	η_{12}	η_{21}	η_{22}
$\frac{dE_1}{dC_1} = 0$	$\frac{dE_1}{dC_2} = 0$	$\frac{dE_2}{dC_1} = 0$	$\frac{dE_2}{dC_2} = 0$
$\frac{dF_1}{dC_1} = 2k_{D1}b_1b_2^2C_{H2} - k_{D2}b_1^2b_2C_{H1}$	$\frac{dF_1}{dC_2} = k_{D1}b_1b_2^2C_{H1}$	$\frac{dF_2}{dC_1} = k_{D2}b_2b_1^2C_{H2}$	$\frac{dF_2}{dC_2} = 2k_{D2}b_2b_1^2C_{H1} - k_{D1}b_2^2b_1C_{H2}$
$\frac{dG_1}{dC_1} = 2k_{D1}b_2^2C_{H2} + b_1b_2^2C_{H1}C_{H2}$ $- b_1b_2^2C_2C_{H1}$ $- 2b_1b_2^2C_1C_{H2}$ $- k_{D2}b_1b_2C_{H1}$	$\frac{dG_1}{dC_2} = -b_1b_2^2C_1C_{H1}$	$\frac{dG_2}{dC_1} = -b_2b_1^2C_2C_{H2}$	$\frac{dG_1}{dC_2} = 2k_{D2}b_1^2C_{H1} + b_2b_1^2C_{H1}C_{H2}$ $- b_2b_1^2C_1C_{H2}$ $- 2b_2b_1^2C_2C_{H1}$ $- k_{D1}b_2b_1C_{H2}$
$\frac{dH_1}{dC_1} = -2b_2^2C_1C_{H2}$	$\frac{dH_1}{dC_2} = 0$	$\frac{dH_2}{dC_1} = 0$	$\frac{dH_1}{dC_2} = -2b_1^2C_2C_{H1}$

Table 3. Dual mode and partial immobilization parameters of the studied polyimides.

Polyimide	T (°C)	Penetrant	D_D (m ² /s)	D_H (m ² /s)	k_D (cm ³ stp/(cm ³ .psia))	b (Psia ⁻¹)	C'_H (cm ³ stp/cm ³)	bC'_H (cm ³ stp/(cm ³ .psia))	F (D_H/D_D)	Refs.
6FDA-6FpDA	35	Propylene	5.96E-10	3.92E-10	0.26	0.24	20.3	4.872	6.58E-01	[44]
		Propane	8.40E-11	8.50E-12	0.20	0.22	11.35	2.497	1.01E-01	
6FDA-6FpDA	70	Propylene	3.45E-09	1.86E-10	0.12	0.32	12.3	3.936	5.39E-02	[44]
		Propane	3.11E-10	3.00E-12	0.10	0.15	9.87	1.480	9.65E-03	
6FDA-DAM	75	Propylene	7.86E-08	7.90E-09	0.15	0.205	17.5	3.587	1.01E-01	[43]
		Propane	9.56E-09	1.53E-09	0.125	0.266	10.7	2.846	1.60E-01	
6FDA-TrMPD	50	Propylene	3.80E-08	4.30E-09	0.265	0.258	26	6.721	1.13E-01	[35]
		Propane	2.50E-09	3.00E-10	0.347	0.476	17	8.095	1.20E-01	

Table 4. The average amounts of frictional coupling effects , membrane sorption level and kinetic coupling effects.

Polyimide	T (°C)	ε_1	ε_2	W_m	B_{average}
6FDA-6FpDA	35	2.99E-07	4.82E-08	0.97	$\begin{bmatrix} 2.6E9 & 0 \\ 0 & 1.69E10 \end{bmatrix}$
6FDA-6FpDA	70	7.72E-08	2.64E-09	0.98	$\begin{bmatrix} 1E10 & 0 \\ 0 & 3.98E11 \end{bmatrix}$
6FDA-DAM	75	3.35E-05	3.89E-06	0.99	$\begin{bmatrix} 2.02E7 & 0 \\ 0 & 1.8E08 \end{bmatrix}$
6FDA-TrMPD	50	2.09E-05	1.20E-06	0.97	$\begin{bmatrix} 3.68E7 & 0 \\ 0 & 6.9E08 \end{bmatrix}$

Table 5. Average values of thermodynamic coupling effects (TCE).

Polyimide	T (°C)	η_{average}
6FDA-6FpDA	35	$\begin{bmatrix} 1.59 & 0.98 \\ 0.3 & 1.46 \end{bmatrix}$
6FDA-6FpDA	70	$\begin{bmatrix} 2.15 & 1.08 \\ 0.43 & 1.41 \end{bmatrix}$
6FDA-DAM	75	$\begin{bmatrix} 1.61 & 0.98 \\ 0.47 & 1.78 \end{bmatrix}$
6FDA-TrMPD	50	$\begin{bmatrix} 1.43 & 0.64 \\ 0.52 & 1.77 \end{bmatrix}$

Table 6. Experimental and optimized diffusion coefficients.

Polyimide	T (°C)	Experimental diffusion coefficients [36, 43] (m ² /s)		Optimized diffusion coefficients using Maxwell-Stefan model without TCE contribution (m ² /s)		Optimized diffusion coefficients using Maxwell-Stefan model with TCE contribution (m ² /s)	
		Propylene	Propane	Propylene	Propane	Propylene	Propane
6FDA-DAM	75	7.86E-8	9.56E-9	6.329E-7	1.25E-8	3.973E-8	9.1E-9
6FDA-TrMPD	50	3.8E-8	2.5E-9	3.279E-8	4.36E-9	2.033E-8	3.16E-9

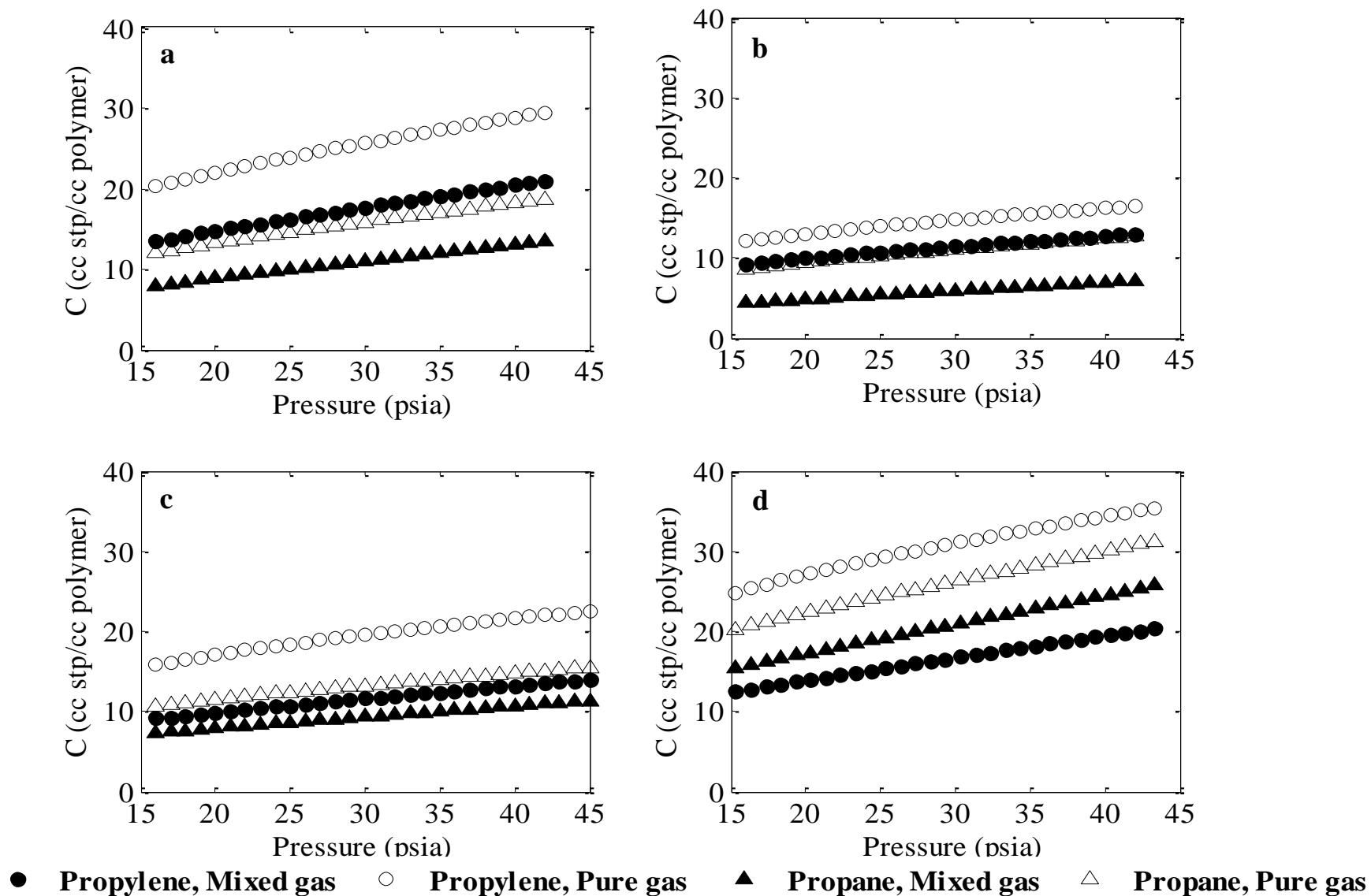


Fig. 1. Pure and mixed gas sorption isotherms in a) 6FDA-6FpDA at 35 °C b) 6FDA-6FpDA at 70 °C c) 6FDA-DAM at 75 °C and d) 6FDA-TrMPD at 50 °C

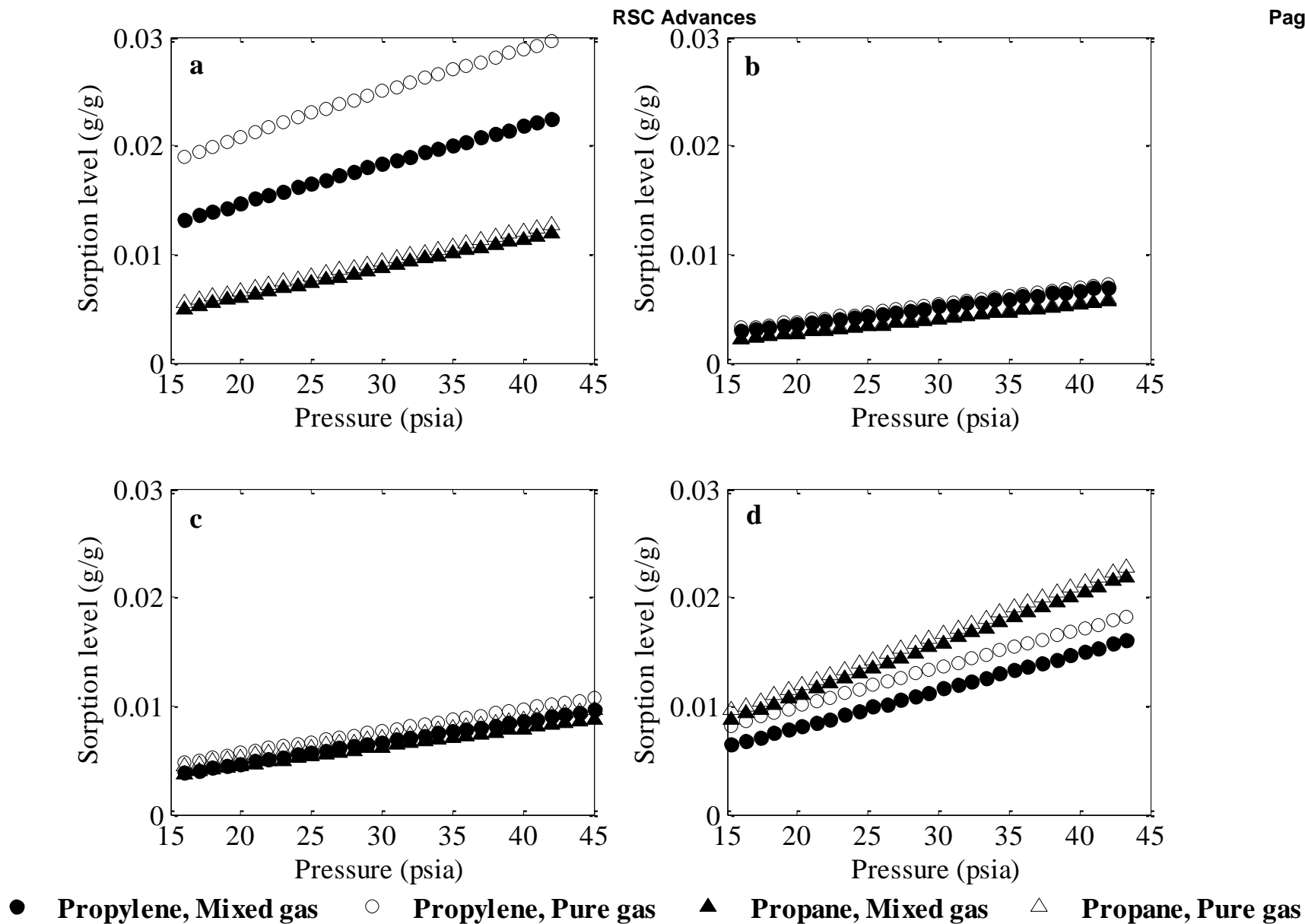


Fig. 2. Pure and mixed gas sorption levels in a) 6FDA-6FpDA at 35 °C b) 6FDA-6FpDA at 70 °C c) 6FDA-DAM at 75 °C and d) 6FDA-TrMPD at 50 °C

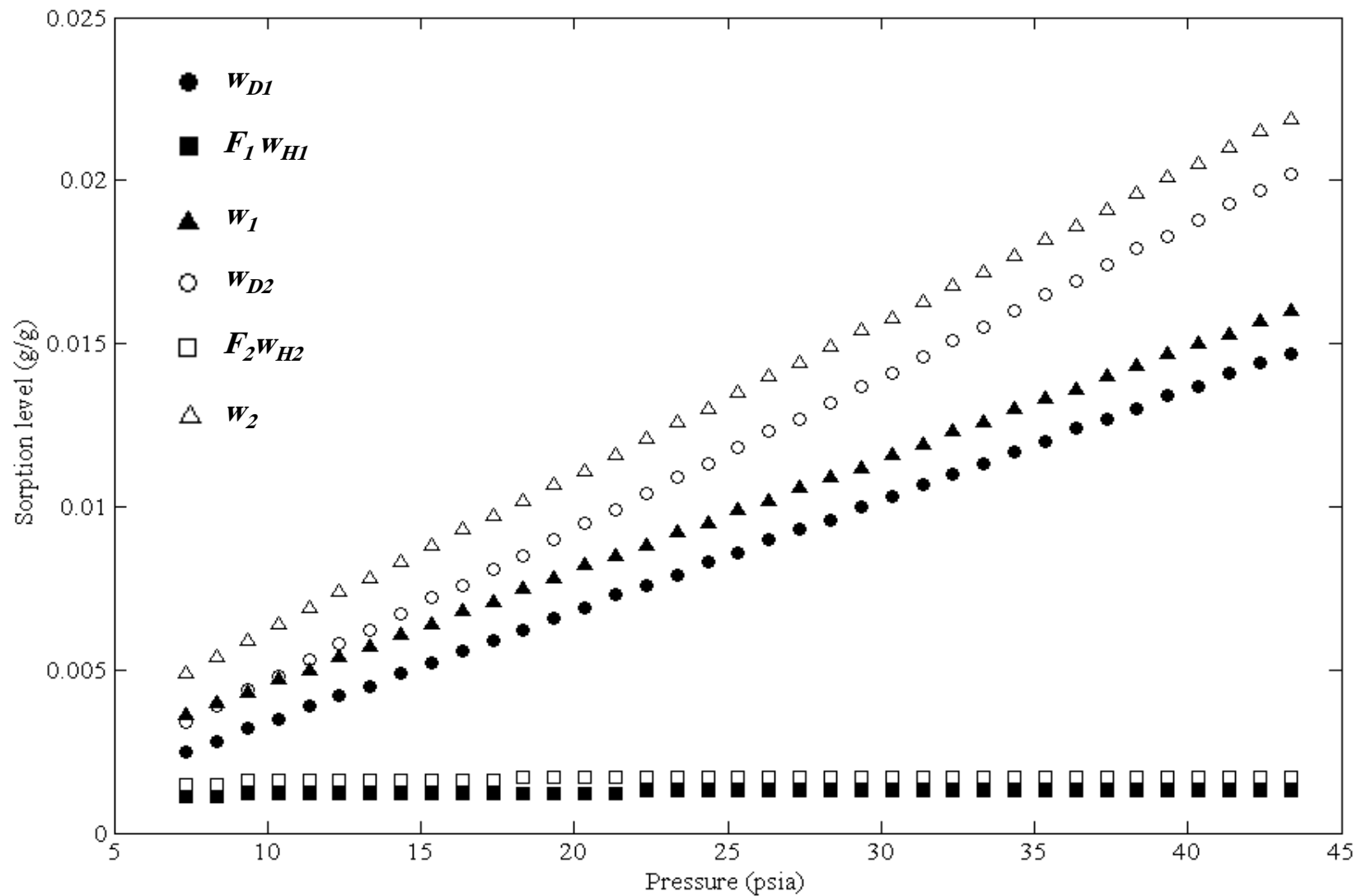


Fig. 3 Parts of mixed gas sorption level in 6FDA-TrMPD at 50 °C

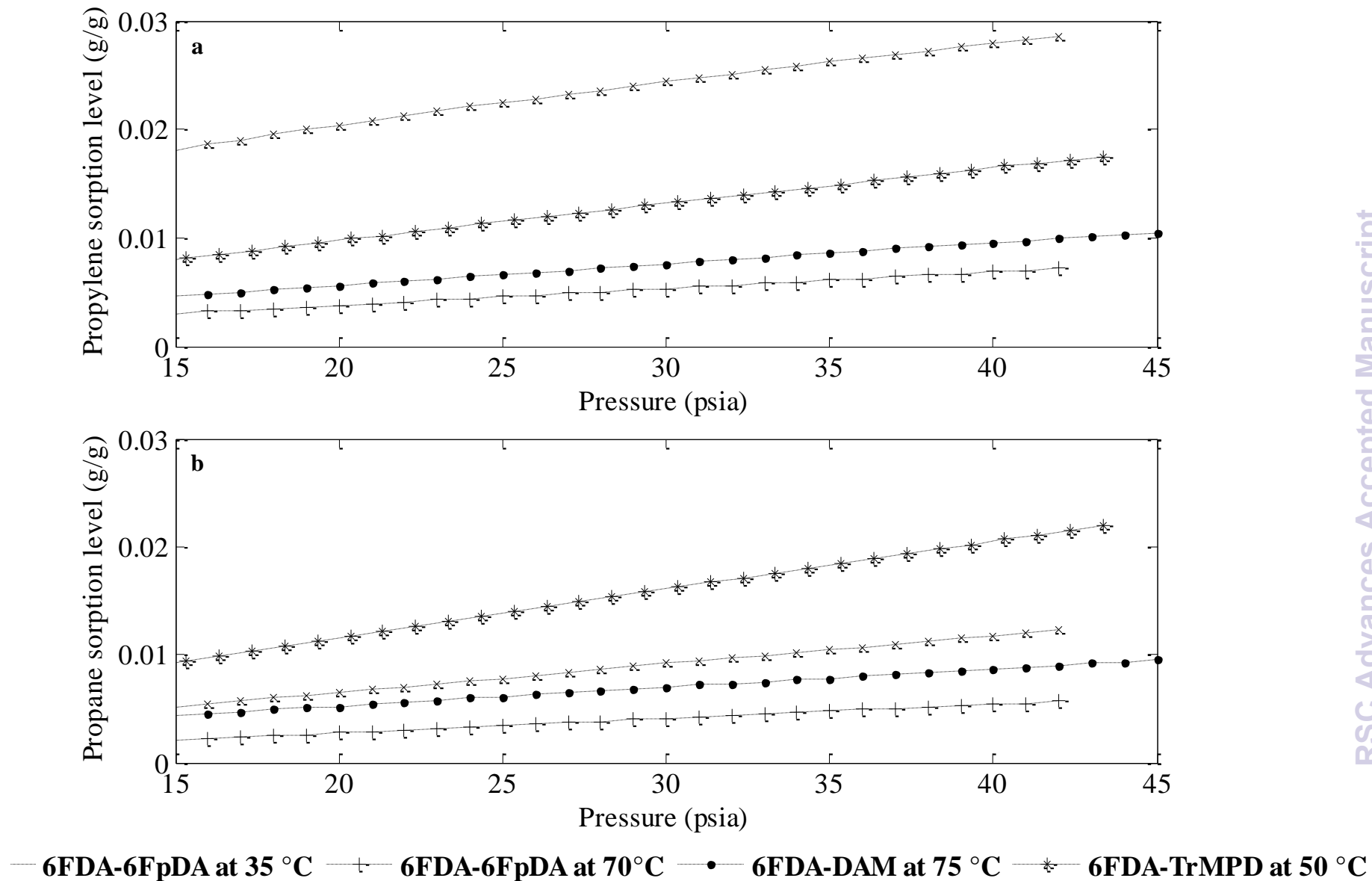


Fig. 4. Sorption levels of a) propylene b) propane in different polyimides

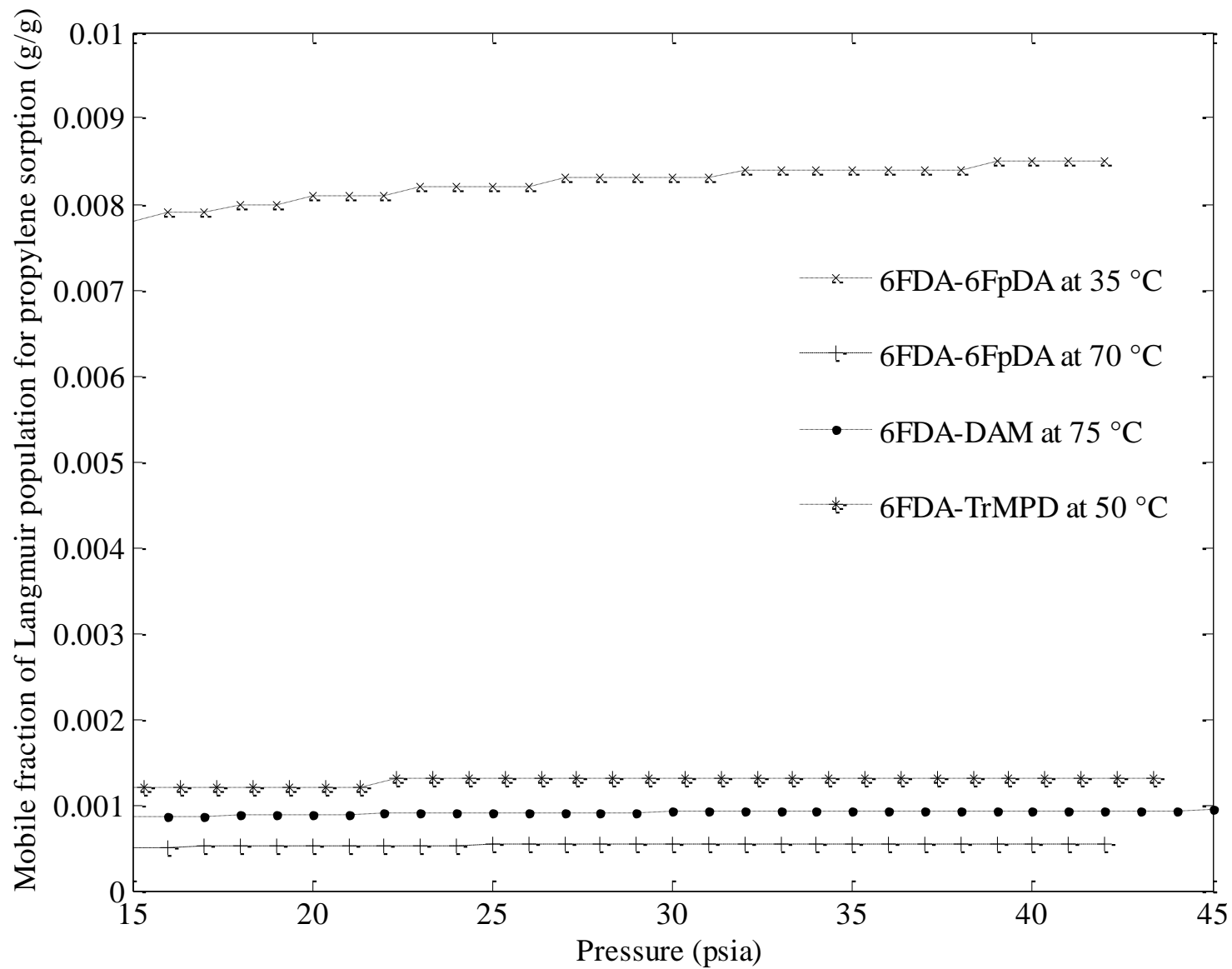


Fig. 5. Mobile fraction of Langmuir population for propylene sorption in different polyimides

RSC Advances

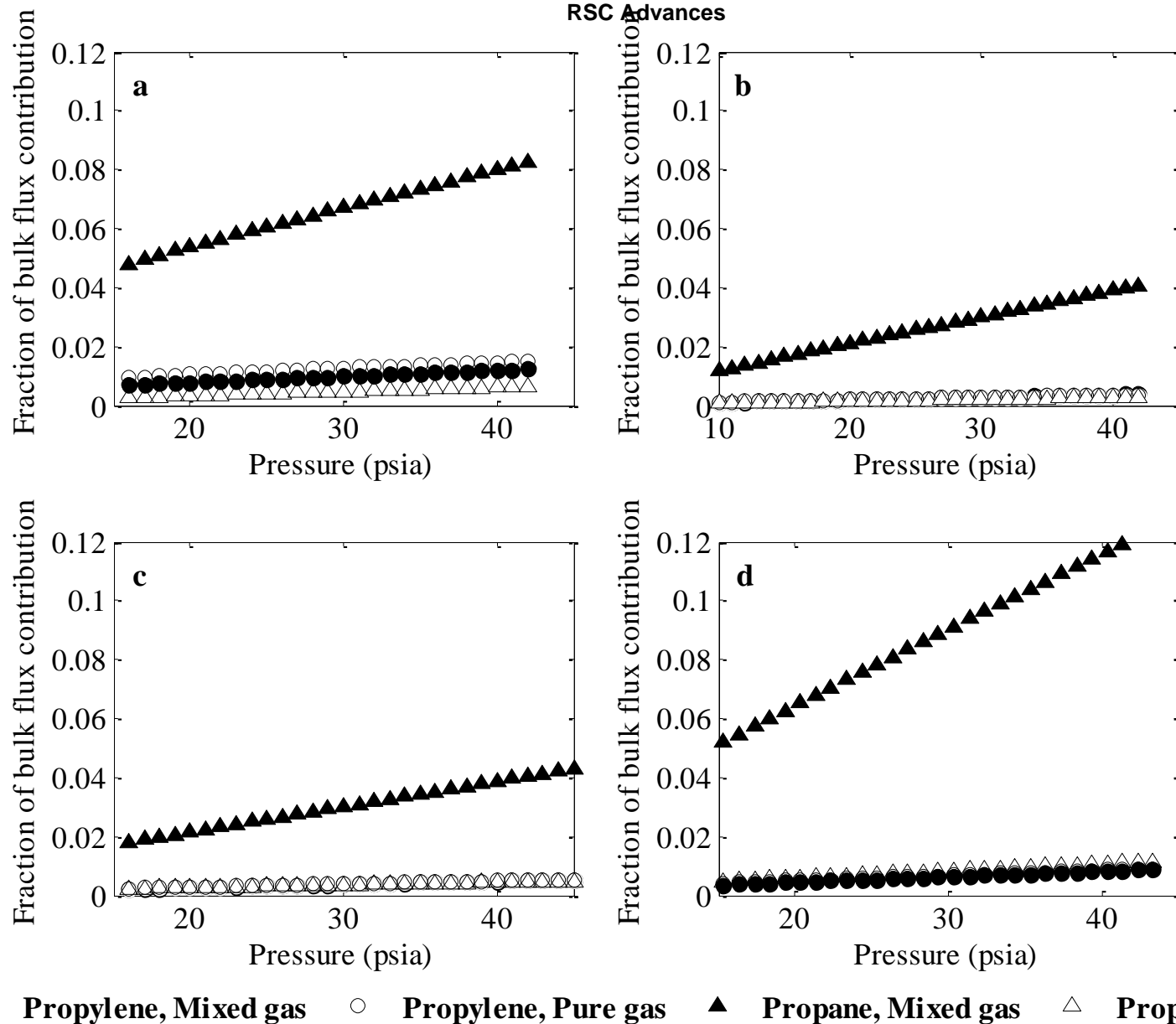


Fig 6. Fraction of bulk flux contribution of propane and propylene in binary mixture compared to the pure gas in a) 6FDA-6FpDA at 35 °C b) 6FDA-6FpDA at 70 °C c) 6FDA-DAM at 75 °C and d) 6FDA-TrMPD at 50 °C

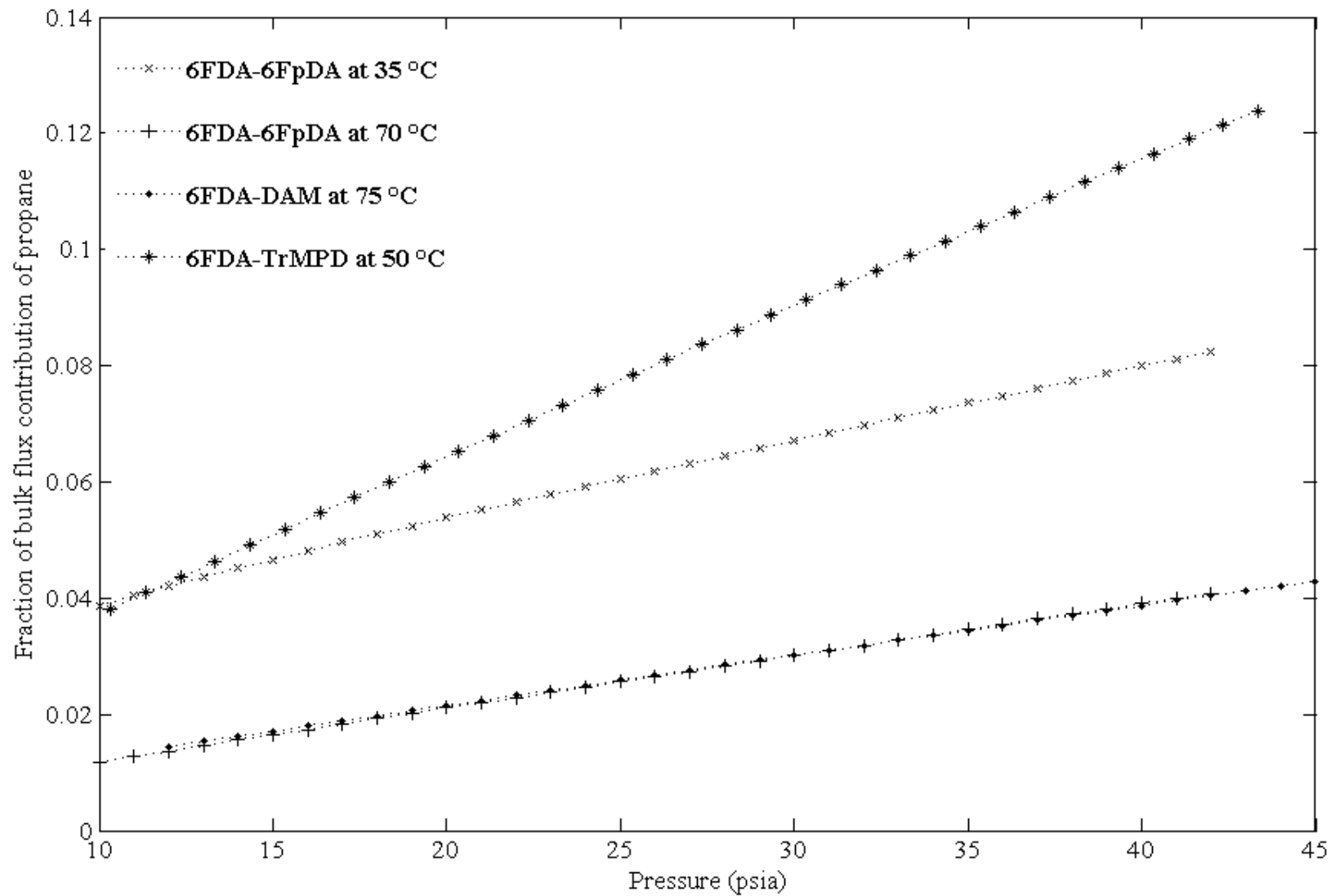


Fig.7. Fraction of bulk flux contribution of propane in different polyimides

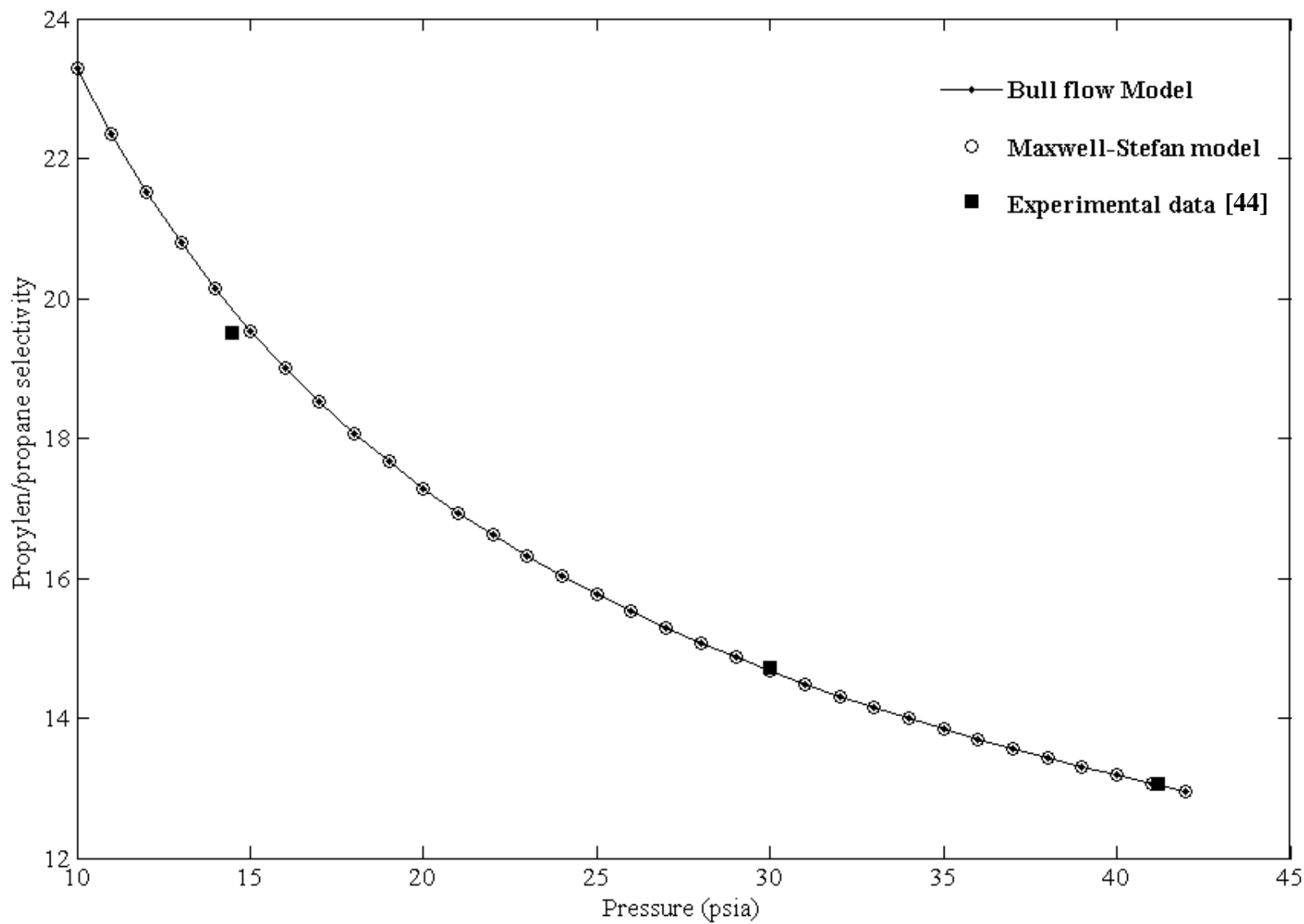
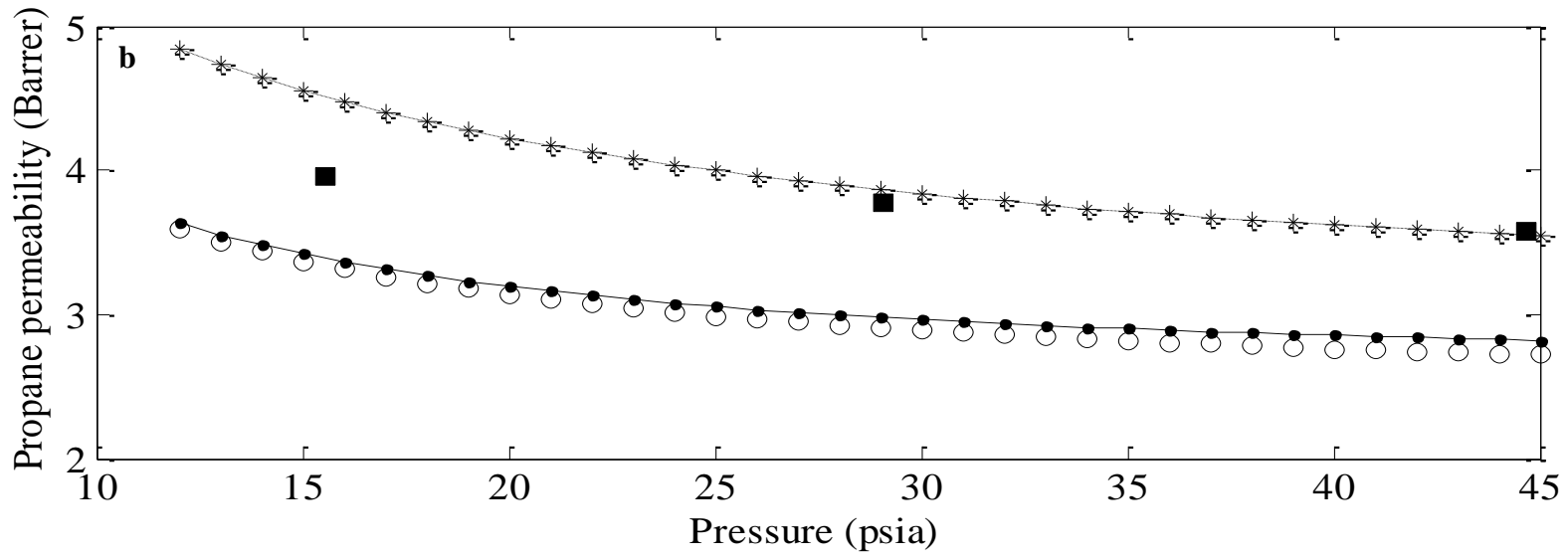
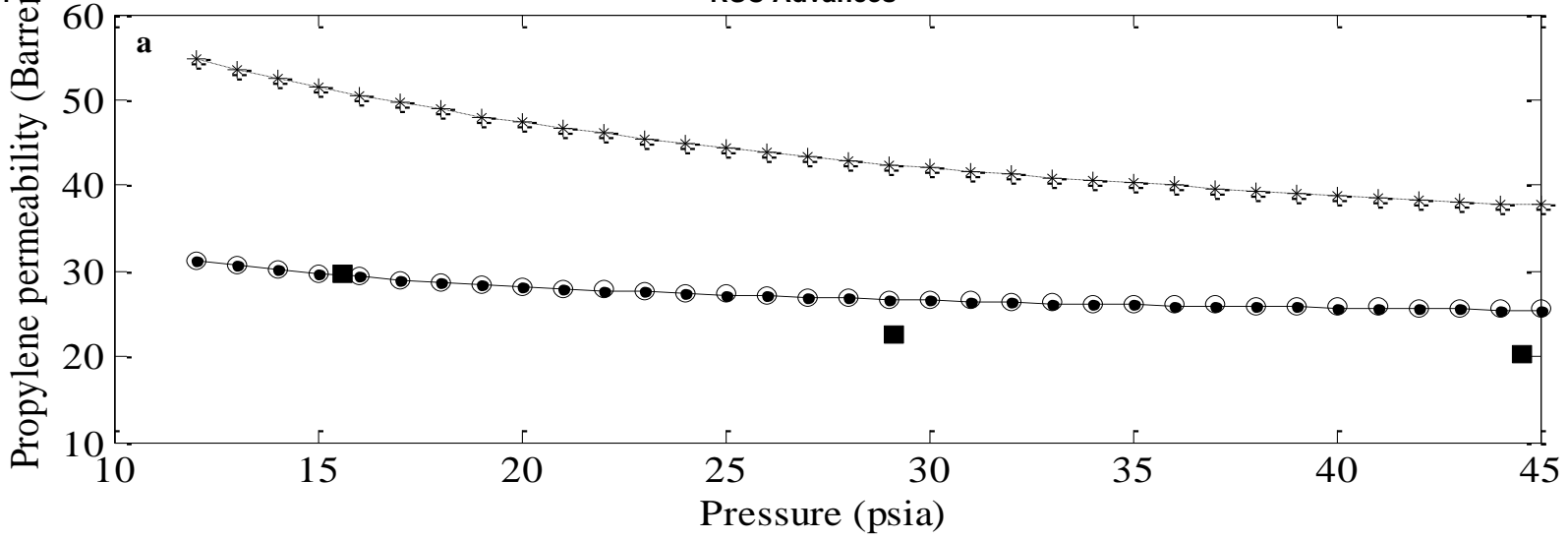


Fig.8. Comparison of experimental and calculated selectivity for 6FDA-6FpDA at 35 °C. (Gas composition 50/50 mol.%)



Bulk flow model
 Maxwell-Stefan model
 Maxwell-Stefan model with TCE contribution
 Experimental data [43]

Fig. 9. Comparison of experimental and calculated permeability of a) propylene and b) propane for 6FDA-DAM at 75 °C. (Gas composition 50/50 mol.%)

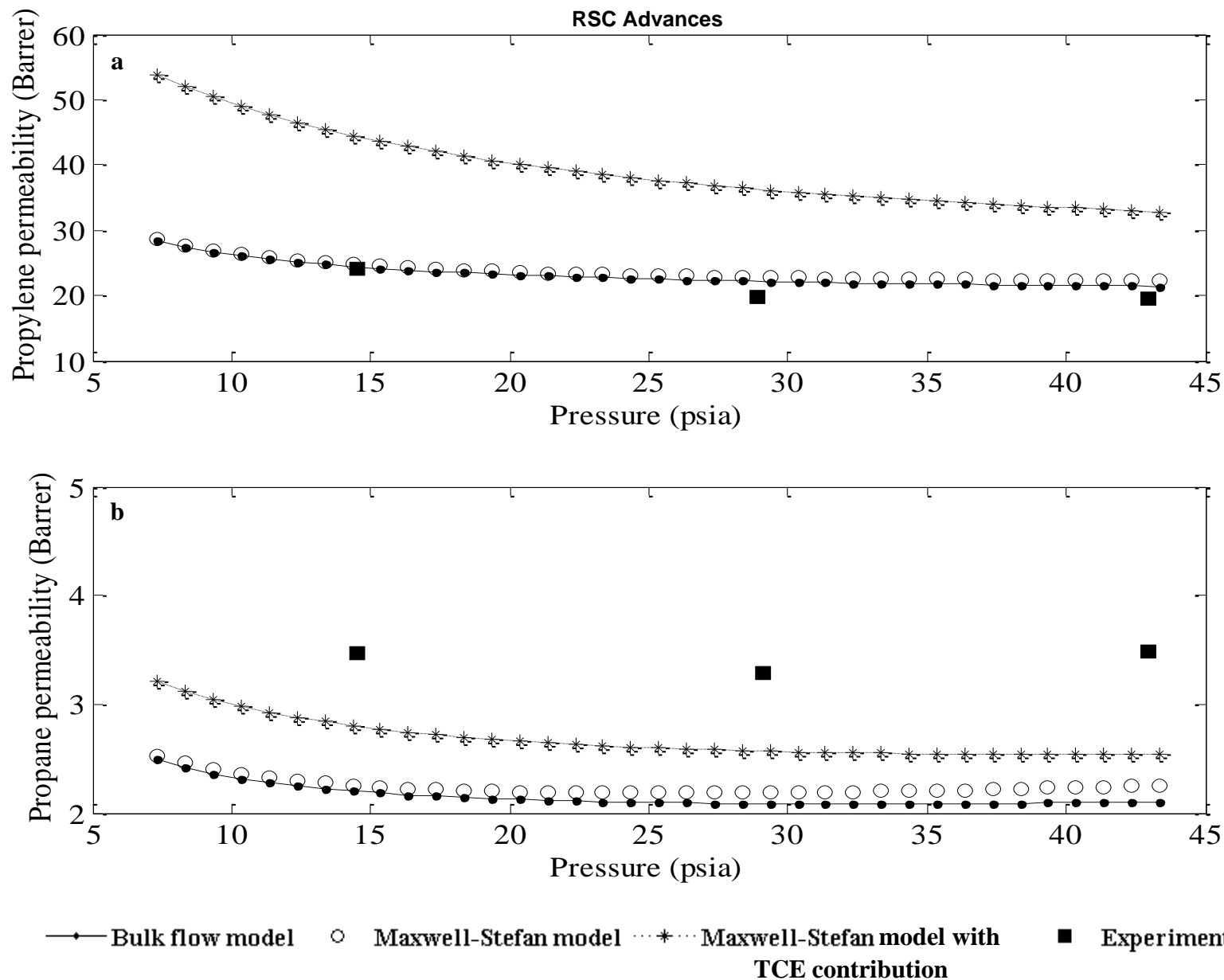


Fig. 10. Comparison of experimental and calculated permeability of a) propylene and b) propane for 6FDA-TrMPD at 50 °C. (Gas composition 50/50 mol.%)

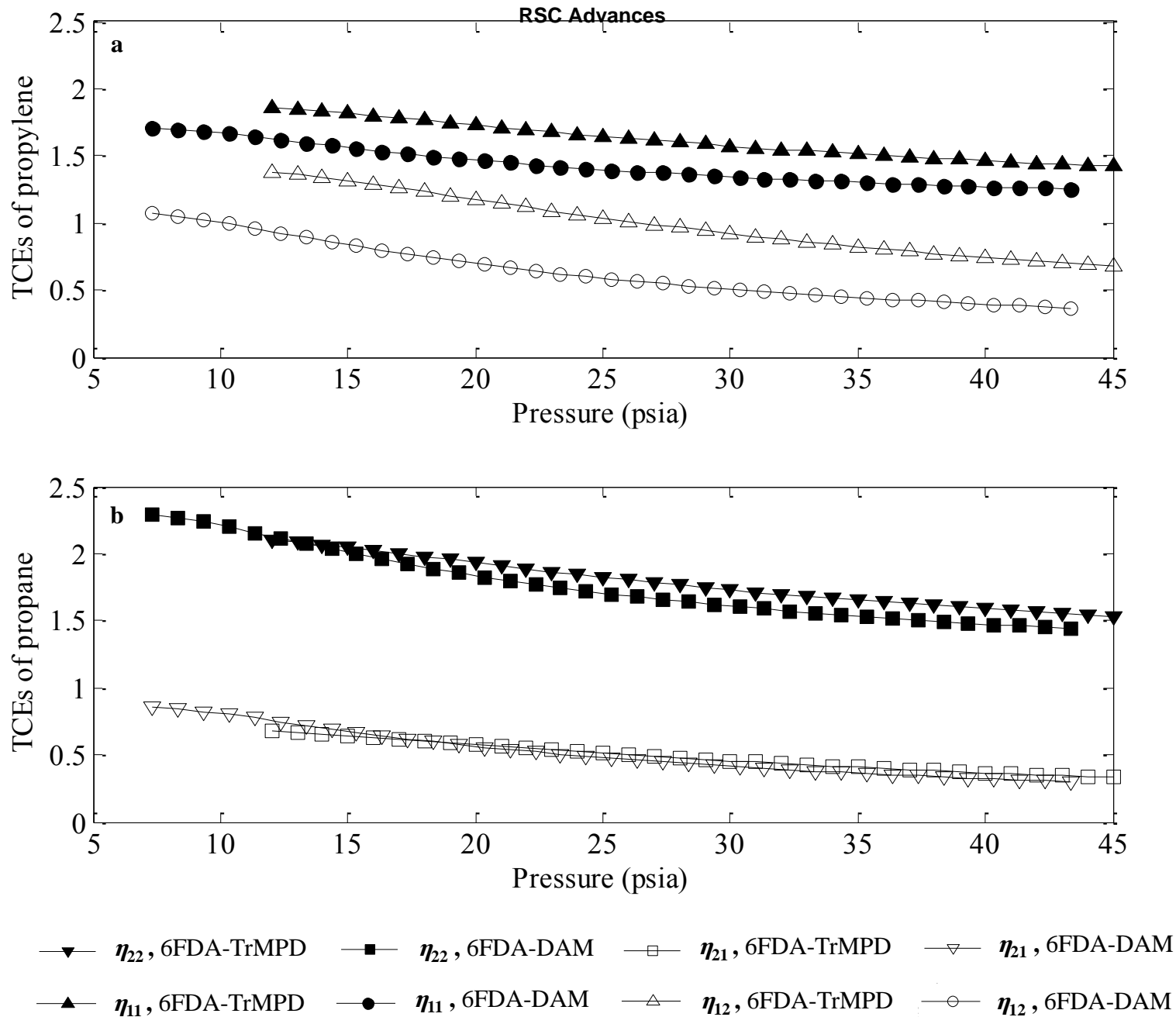


Fig. 11. Thermodynamic coupling effects of a) propylene and b) propane (Gas composition 50/50 mol.%)

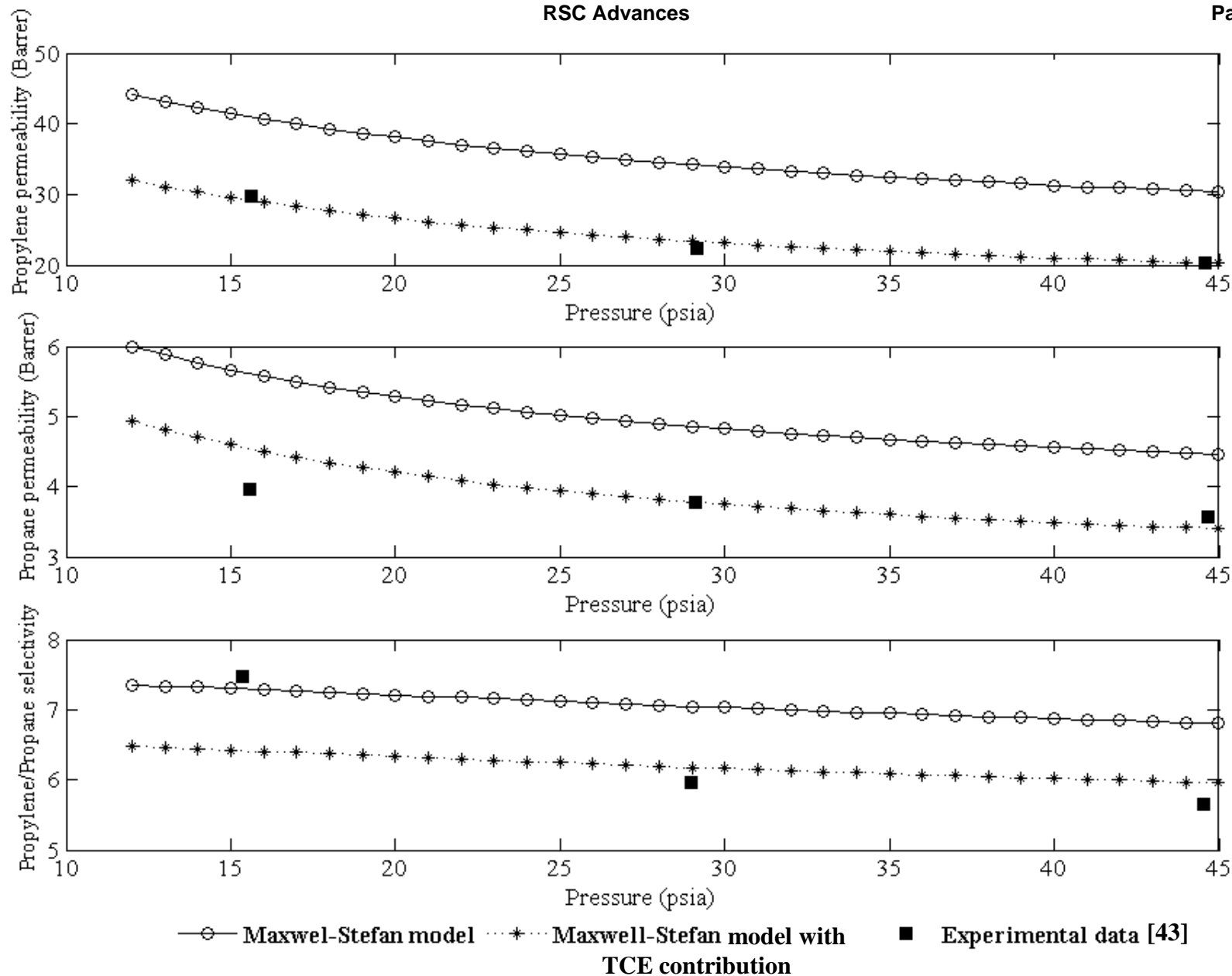


Fig. 12. Predictions of the Maxwell-Stefan model without and with TCE contribution using optimized diffusion coefficients for 6FDA-DAM at 75 °C. a) propylene permeability and b) propane permeability c) propylene/propane selectivity (Gas composition 50/50 mol.%)

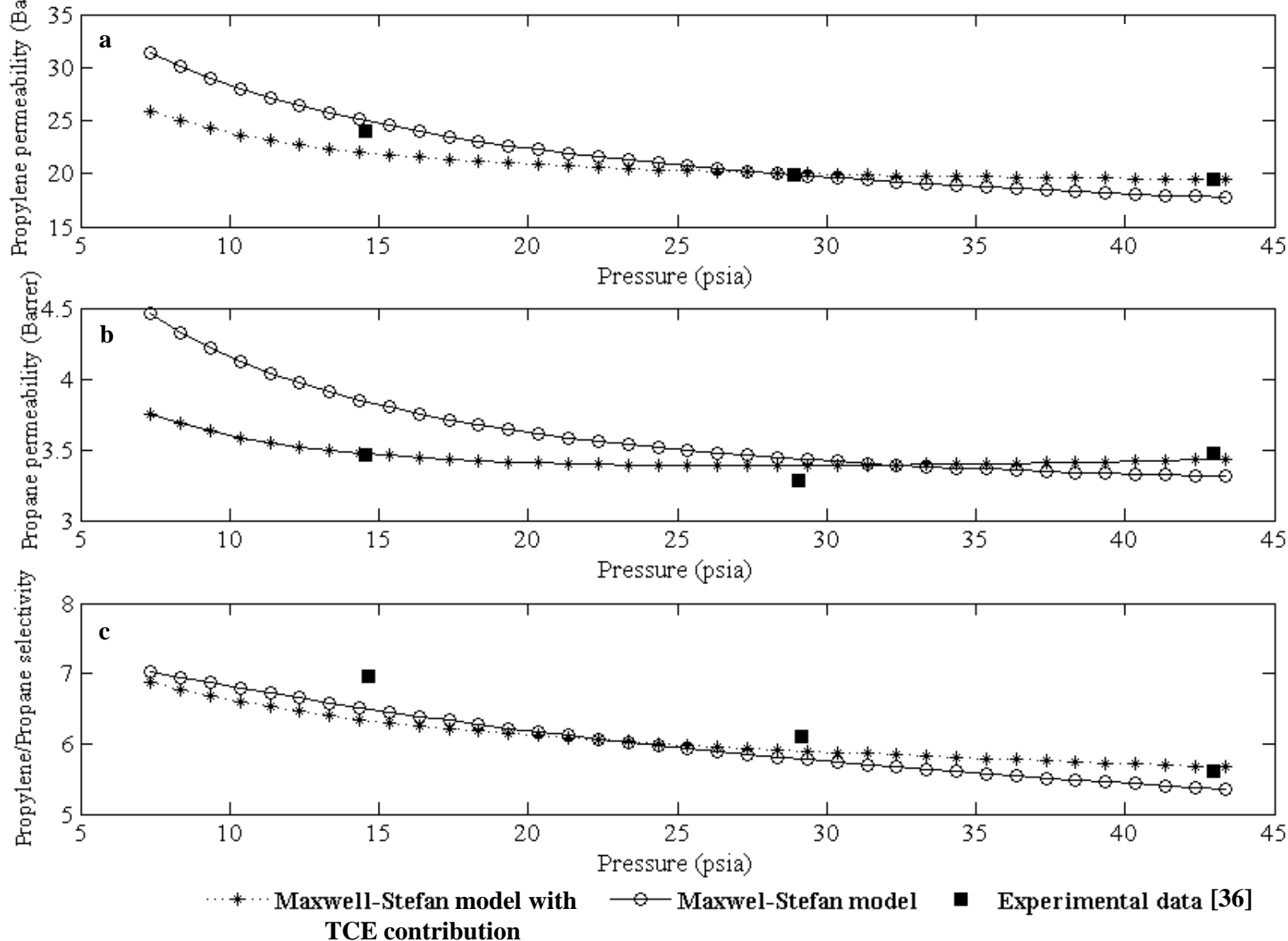


Fig. 13. Predictions of the Maxwell-Stefan model without and with TCE contribution using optimized diffusion coefficients for 6FDA-TrMPD at 50 °C. a) propylene permeability and b) propane permeability c) propylene/propane selectivity (Gas composition 50/50 mol.%)